Distinct Chemical Factors in Hydrolytic Reactions Catalyzed by Metalloenzymes and Metal Complexes

Journal:	*ChemComm*
Manuscript ID	CC-FEA-03-2023-001380.R1
Article Type:	Feature Article

SCHOLARONE™
Manuscripts

1

Distinct Chemical Factors in Hydrolytic Reactions Catalyzed by Metalloenzymes and Metal Complexes

Leonardo F. Serafim, Vindi M. Jayasinghe-Arachchige, Lukun Wang, Parth Rathee,

Jiawen Yang, Sreerag N. Moorkkannur, and Rajeev Prabhakar*

Department of Chemistry, University of Miami, Coral Gables, FL 33146

* To whom correspondence should be addressed; rpr@miami.edu; Tel: 305-284-9372;

Fax: 305-284-4571.

Abstract. The selective hydrolysis of the extremely stable phosphoester, peptide and ester bonds of molecules by bio-inspired metal-based catalysts (metallohydrolases) is required in a wide range of biological, biotechnological and industrial applications. Despite the impressive advances made in the field, the ultimate goal of designing efficient enzyme mimics for these reactions is still elusive. Its realization will require a deeper understanding of diverse chemical factors that influence activities of both natural and synthetic catalysts. They include catalyst-substrate complexation, non-covalent interactions and the electronic nature of the metal ion, ligand environment and nucleophile. Based on our computational studies, their roles are discussed for several mono- and binuclear metallohydrolases and their synthetic analogues. Hydrolysis by natural metallohydrolases is found to be promoted by a ligand environment with low basicity, a metal bound water and a heterobinuclear metal center (in binuclear enzymes). Additionally, peptide and phosphoester hydrolysis are dominated by two competing effects *i.e.* nucleophilicity and Lewis acid activation, respectively. In synthetic analogues, hydrolysis is facilitated by the inclusion of a second metal center, hydrophobic effects, a biological metal (Zn, Cu and Co) and a terminal hydroxyl nucleophile. Due to the absence of protein environment, hydrolysis by these small molecules is exclusively influenced by nucleophile activation. The results gleaned from these studies will enhance understanding of fundamental principles of multiple hydrolytic reactions. They will also advance the development of computational methods as a predictive tool to design more efficient catalysts for hydrolysis, Diels-Alder reaction, Michael addition, epoxide opening and aldol condensation.

I. Introduction. The design of small metal complexes that can efficiently mimic the activities of metalloenzymes has been one of the holy grails in chemistry.[1-8] In the last few decades, a wide range of complexes has been designed to selectively catalyze diverse chemical reactions.[9-38] They were by and large inspired by mono- and binuclear metal centers of enzymes.[30, 39-53] Despite the substantial progress made in the field, the existing metal complexes exhibit much slower activities and lower turnover numbers in comparison to natural enzymes. Therefore, there is an intense interest in the development of the next generation of molecules with enhanced activities.[4, 5, 7, 29, 30, 54-62] Based on our research, this article is focused on mechanisms of different metalloenzymes and their synthetic analogues that promote hydrolysis of peptide (-(O=)C-NH-), ester ((R)(C=O)(OR)) and phosphoester ((O=)(RO)(RO)(P-O-R)) bonds. Specifically, the roles of distinct chemical factors such as metal ion(s), ligand environment, nature of substrates, coordination numbers and non-covalent interactions that control their functioning are elucidated. An improved understanding of these factors will help in the design of versatile catalysts not only for hydrolysis but many other reactions including epoxide opening, aldol condensation, Michael addition and Diels-Alder reactions.[63-67]

The peptide, ester and phosphoester bonds are ubiquitous in a wide range of biologically, industrially and environmentally relevant molecules such as proteins, pharmaceuticals, deoxyribonucleic acid (DNA), pesticides, nerve agents and plastic products.[14, 68-70,12, 71-74,75-77] As a result, their selective hydrolysis plays important roles in many critical applications like protein engineering, therapeutics, genomics, DNA repair and remediation of pesticides, nerve agents and plastics.[78-84] As expected these bonds are extremely stable and the half-life for the hydrolysis of peptide, ester and phosphoester bonds is 350-600, 60-470 and ~130,000 years, respectively, at

room temperature and pH = 4-8.[85, 86] In nature, these bonds are hydrolyzed by highly specialized mono-and binuclear metal center containing enzymes that depending on the nature of the scissile bond are categorized as proteases/peptidases, esterases and phosphatases/nucleases and in general known as metallohydrolases.[12, 14, 69, 70, 87-93] These bonds can also be cleaved by a wide range of organic cofactor possessing enzymes.[94] For instance, serine proteases, cysteine proteases, threonine proteases, glutamic proteases, and aspartyl proteases utilize either a triad or dyad formed by specific amino acid residues to hydrolyze peptide bonds of their substrates.[95, 96] Metallohydrolases display significant structural diversity in terms of amino acid sequence, nature of metal ions and substrates, ligand environment and second coordination shell residues. Therefore, it is of fundamental importance to develop a deeper understanding of their reaction mechanisms. In these mechanisms, a multitude of chemical factors such as the nature of metal center (mono- or binuclear), metal ions (di-, tri or tetravalent), ligand environment (symmetric or asymmetric), catalyst-substrate complexation (monodentate, bidentate or indirect), nucleophile (terminal or bridging) and non-covalent interactions play key roles. These distinct factors are productively utilized by these catalysts for their efficient functioning. However, their sources, extent and combinations are system dependent and it is not trivial to separate and elucidate them experimentally.[29, 97-101] The available experimental information provided an ideal platform to employ our theoretical and computational chemistry techniques to understand their roles in these reactions.

II. Mechanisms of natural metallohydrolases and their synthetic analogues. In this section, the aforementioned effects are systematically discussed for peptide, ester and phosphoester hydrolysis. These effects include substrate and water activation, nucleophilicity, basicity and metal

cooperativity and discussed using the computed values of the scissile bond, O-H of water, metal-nucleophile, metal-ligand and metal-metal distances as parameters.

IIa. Peptide hydrolysis by metalloproteases. Here, mechanisms of different mono- [insulin degrading enzyme (**IDE**), neprilysin (**NEP**) and matrix metalloproteinase (**MMP**)] and binuclear [bovine lens leucine aminopeptidase (**BILAP**) and *Streptomyces griseus* aminopeptidase (*Sg*AP)] metalloproteases are discussed (Figure 1). **IDE** contains a common $Zn-N_2O$ [Zn-(His, His and Glu)] catalytic core that is also possessed by other members of the family such as thermolysin (TLN) and carboxypeptidase A (Figure 1).[89, 102-106] It catalyzes the degradation of several critical biomolecules like insulin, amyloid beta (Aβ), amylin and glucagon.[89] This enzyme plays a preventive role in the development of cancer, obesity, Alzheimer's disease (AD) and type-2 diabetes.[107, 108] It exhibits broad specificity and hydrolyzes a wide range of chemically diverse peptide bonds of its substrates like Val-His, His-Gln, Phe-Phe and Lys-Gly of Aβ.[89, 109, 110] **NEP** is also a $Zn-N_2O$ [Zn-(His, His and Glu) in Figure 1] core possessing enzyme that hydrolyzes a variety of physiologically relevant molecules including Aβ, leucine[5] or methionine[5]-enkephalin, bradykinin, atrial natriuretic factor (ANF) and substance P.[111-113] It exhibits a preference for cleavage on the amino terminal side of hydrophobic residues. In comparison to **IDE** and **NEP**, **MMP**[114, 115] possesses a $Zn-N_3$ [Zn-(His, His and His)] core in which a negatively charged Glu residue is substituted with a neutral His residue (Figure 1). This core is also commonly found in other matrix metalloproteinases[116, 117] and carbonic anhydrase[118, 119]. **MMP** degrades collagen, elastin, gelatin, and other glycoproteins and proteoglycans.[114] It is involved in cardiovascular diseases and many different types of cancers.[120, 121] Among binuclear metallohydrolases, a non-equivalent $Zn1(O_3)-Zn2(NO_3)$ [Zn1(Asp, Glu, Asp)-Zn2(Lys, Glu, Asp, Asp)] core containing

BILAP is extremely prevalent and found in humans, animals, bacteria, and plants (Figure 1).[9, 70] It prefers to hydrolyze a leucine residue located at the N-terminus in a di- or tripeptide sequence, but also is capable of hydrolyzing other amino acids as well.[40] **BILAP** has been implicated in HIV, cancer, cataract, and cystic fibrosis.[122] On the other hand, **SgAP** contains an almost equivalent $Zn1(NO_2)$-$Zn2(NO_2)$ [Zn1(His, Asp and Asp)-Zn2(His, Glu, and Asp)] core and exhibits exceptional catalytic promiscuity by hydrolyzing both peptide and phosphoester bonds with remarkable efficiency (Figure 1).[123, 124] It exhibits a preference for large hydrophobic N-terminus residues and can hydrolyze different amino acid (Gly, Met, Val, Ala, Lys) - *p*NA (para-nitro aniline) analogues.[124] Thus, due to their structural and catalytic properties, these enzymes serve as model systems to gain deeper understanding of peptide hydrolysis by metalloproteases.

All these enzymes follow the general acid/base mechanism(s) for the hydrolysis of different substrates (Figure 2). In the first step of the mechanism for mononuclear enzymes (Figure 3a), a water molecule is activated by a base to create the hydroxyl nucleophile. It could be generated by using either a metal bound or free water molecule and Glu, Asp or His-Asp dyad as a base in these systems. In the second step, the nucleophile generated in the previous step attacks the scissile peptide bond (C-N) of the substrate and creates a tetrahedral *gem*-diolate intermediate. In some cases, the first two steps could also occur synchronously in a single step. In the final step, the cleavage of the C-N bond through a proton abstraction by the substrate collapses the intermediate. This process can also occur through distinct pathways in these enzymes. A vast majority of metalloproteases contain the Zn^{2+} ion due to its high Lewis acidity, a redox-inactive state, low ligand field stabilization energy, and flexible coordination number (3-5).[125] These properties facilitate activation of the substrate, creation of the nucleophile and release of the product. In the

section below, the information concerning the roles of diverse chemical factors in these steps of

the aforementioned metalloproteases derived from quantum chemical calculations is discussed.

Almost all structures in DFT calculations discussed below were optimized using the hybrid B3LYP

functional[126, 127] and double zeta basis set. The energetically most feasible mechanisms were also

investigated using other functionals such as MPW1PW91[128] and M06-2X[129]. The small energy

differences (1.0 – 2.0 kcal/mol) between different functionals showed that energies were not very

sensitive to the level of theory used in these calculations.

IIa1. Generation of the nucleophile and gem-diolate intermediate. Here, a metal bound water

is commonly used to create the hydroxyl nucleophile (Figure 3a). Its binding to a metal ion and

hydrogen bonding by a neighboring negatively charged amino acid residue lower its pK_a value

from ~14 to ~7.[130, 131] This is a common strategy utilized by metallohydrolases to activate a water

molecule. A vast majority of these enzymes possess Zn at their active sites.[132] A low coordination

number (3-4) of Zn^{2+} in these sites increases the acidity of a water molecule and promote the

formation of the hydroxyl nucleophile.[125] It is noteworthy that non-metallic proteases that contain

only an organic cofactor activate a free water utilizing only non-covalent interactions.[88, 133, 134] In

the reactant of **IDE**, the Zn^{2+} metal ion is coordinated to three direct ligands (His, His and Glu), a

nucleophile generating water molecule and the substrate through the Zn-carbonyl bond. In a

concerted manner, a second coordination shell Glu residue functions as a base and triggers the

nucleophilic attack on the substrate to generate the gem-diolate intermediate. Rather interestingly,

the computed energetics predicts that this step depends on the nature of the substrate. For instance,

it occurs with barriers of 14.3, 18.8 and 22.3 kcal/mol for three chemically distinct dipeptides Lys–

Gly (polar-nonpolar), Phe–Phe (nonpolar-nonpolar), and His–Gln (polar-polar) substrates,

respectively.[135] The modes of substrate binding and alterations in the metal-substrate and metal-water bonds contributes to the differences in computed barriers. These interactions provide measures of Lewis acid and nucleophile activations by the metal center. The computed barriers are in line with the measured value of 17.2 kcal/mol for Aβ degradation by **IDE**.[110] Additionally, it is comparable to the measured (12.4-16.3 kcal/mol)[136] and calculated (15.2 kcal/mol)[131] barriers for thermolysin. Furthermore, this step is identified as the rate-limiting step of the entire mechanism for all three substrates. In the gem-diolate intermediate, the scissile peptide bond is significantly activated for all three substrates in comparison to the corresponding reactant.

NEP that also possesses the **IDE** like $Zn-N_2O$ core interacts with the polyethylene terephthalate (PET) substrate (Figure 2), an ester, through the metal-carbonyl bond. However, in comparison to **IDE**, this enzyme can utilize either a metal bound or free water for hydrolysis (Figure 3a).[137] In the reactant of **NEP**, as discussed for **IDE**, the metal-bound water is significantly activated (1.04 Å) due to the combined polarization by the Zn^{2+} ion and Glu base. It readily donates its proton to Glu and the hydroxyl nucleophile concomitantly attacks the substrate. The barrier of 9.1 kcal/mol for this step is substantially lower than barriers computed for all three substrates of **IDE** due to the provision of a stronger nucleophile by the enzyme. However, in an alternative pathway, a non-metal bound water is activated by the His-Asp dyad base, instead of a Glu residue in the previous pathway, to create the nucleophile. In the reactant, the nucleophile generating water interacts with the His residue of the dyad through a strong hydrogen bond. It is noteworthy that the Asp residue of the dyad facilitates the proton abstraction by the His residue. Here, the water activation (0.99 Å) is significantly less than the one obtained upon metal binding. However, the addition of a hydrogen bond to the nucleophile generating water by an external water further increases its acidity

and elongates the O-H bond by an additional 0.01 Å. It is still less activated than the water (1.04

Å) upon metal binding. Here, the nucleophile attack takes place with a barrier of 13.9 kcal/mol

that is 4.8 kcal/mol higher than the corresponding barrier for the attack by the metal-bound

hydroxyl. This increase is attributed to the provision of a weaker nucleophile in the pathway. On

the other hand, **MMP** utilizes a slightly different $Zn-N_3$ core formed by three neutral His ligands

(Figure 1).[114, 138] In the reactant of **MMP**, the metal-ligand bonds are longer than in the **IDE** case.

Additionally, the metal-substrate interaction is weaker, while the metal-water coordination is

stronger in comparison to the N_2O core containing **IDE**.[139] The computed barrier is 3.4 kcal/mol

lower than the **IDE** case *i.e.* 15.4 kcal/mol from the corresponding reactant for the same Phe-Phe

substrate. However, unlike **IDE**, creation of the gem-diolate intermediate takes place in a stepwise

manner for this enzyme. It shows that a single substitution in the metal center shifted the rate-

determining step of the mechanism.

These results elucidate that the metal-bound water is more activated than a free water polarized by

non-covalent interactions. However, inclusion of a hydrogen bond enhances its acidity. Due to the

difference in acidity of water, the basicity of Glu or the His-Asp dyad cannot be compared. The

lower basicity of the ligand environment of **MMP** also influences the energetics of the mechanism.

In comparison to mononuclear metallopeptidases, their binuclear counterparts such as **BILAP** and

***Sg*AP** follows a mechanism in which both nucleophile and gem-diolate intermediate generation

occurrs in a concerted manner (Figure 3b). **BILAP** utilizes a non-equivalent binuclear core

$Zn1(O_3)-Zn2(NO_3)$ for hydrolysis (Figure 1). In the reactant, similar to mononuclear enzymes, the

L-leucine-*p*-nitroanilide substrate (Figure 2) directly interacts with the Zn1 ion through the

carbonyl group of the scissile peptide bond.[140] In contrast to them, the nucleophile generating water molecule bridges (μ-OH_2) both metal ions and is more acidic. However, in the creation of the gem-diolate intermediate the nucleophile is provided by only one metal center. The greater nucleophilicity of a single metal bound hydroxyl group in comparison to the μ-OH_2 mode is likely to be the reason for that. In this enzyme, there are two candidates to play the role of a base, a Zn2-bound Asp residue and a bicarbonate ion. The former has been proposed as a base in theoretical studies of other members of the family such as *Aeromonas proteolytica* aminopeptidase (AAP),[141] methionine aminopeptidase (MetAP),[142] and prolidase[143] that lack the bicarbonate ion. In **BILAP**, the formation of the gem-diolate intermediate is found to take place through a similar barrier of ~19.0 kcal/mol using either metal bound Asp or the bicarbonate ion as the base. The substitution of L-leucine-*p*-nitroanilide possessing an electron withdrawing nitro group (-NO_2) with L-leucyl-*p*-anisidine (Figure 2) that contains an electron donating methoxy group (-OCH_3) shortens both metal-nucleophile and scissile peptide bonds by 0.02 Å. These changes weaken the nucleophile and strengthen the peptide bond. As a result, the barrier is increased by 7.5 kcal/mol in comparison to the L-leucine-*p*-nitroanilide substrate. Furthermore, replacement of Zn1 and Zn2 with Mg and Co in the Mg1-Zn2 and Mg1-Co2 variants, on the basis of experiments,[144] reduce both the metal-nucleophile and metal-substrate distances. The barrier for this step decreases slightly by 2.0 kcal/mol for the Mg1-Zn2 enzyme and increases by 6.9 kcal/mol for the Mg1-Co2 enzyme.

*Sg*AP possesses an almost equivalent binuclear core, Zn1(NO_2)-Zn2(NO_2) (Figure 1) in comparison to a non-equivalent core of **BILAP**. The theoretical calculations propose a hybrid mechanism for the Leu-*p*NA (Figure 2) hydrolysis catalyzed by the enzyme.[145] In the reactant, both functional groups (carbonyl and amine) of Leu-*p*NA interact with the binuclear metal core

i.e. the amine group coordinates to Zn1, while the carbonyl group to Zn2. Additionally, similar to

BILAP, the nucleophile generating water is symmetrically bound in the μ-OH manner to both

metals. This binding mode was also in agreement with the fluoride inhibition experiments.[146] The

hydrogen bonding of the water with two second coordination shell Glu residues leads to a much

greater activation (O-H = 1.05 Å) in comparison to its terminal bound form (O-H = 1.02 Å). The

strengthening of the scissile peptide bond by 0.03 Å in comparison to the corresponding bond in

its free form suggests the complete absence of its Lewis acid activation. In the reactant, the

bridging water form transforms into the terminal form by switching to the Zn1 site to adopt a more

reactive conformation. The terminal form is 5.1 kcal/mol endergonic from the reactant. From the

terminal form, the nucleophile generation through a proton transfer to the Glu base and

simultaneous attack on the substrate occurr with a barrier of 14.1 kcal/mol (Figure 3b). A five-

membered ring containing intermediate formed in the process is almost thermoneutral (exergonic

by 1.4 kcal/mol). As proposed by the site-directed mutagenesis experiments,[147] this intermediate

is stabilized by a Tyr residue.

These results predict that the water is significantly more activated in bridging binding mode in

comparison to the terminal binding mode. This process is predominantly controlled by the

nucleophilicity of the hydroxyl ion. Additionally, the electronic nature of the substrate influences

the energetics of the step *i.e.* an electron donating group in L-leucine-*p*-nitroanilide is more

amenable to hydrolysis by **BILAP**. The Mg-Zn variant of **BILAP** is more active than its wild-type

form (Zn-Zn).

IIa2. Cleavage of the peptide bond: This process occurs through the collapse of the gem-diolate intermediate created in the previous step (Figure 3a).

In **IDE**, Glu acts as both acid and base by abstracting the proton from the metal bound oxygen atom of the intermediate and donating its previously acquired proton to the peptide bond. This double proton transfer cleaves the peptide bond. Similar to the previous step, with the barriers of 9.2, 13.9 and 18.5 kcal/mol a clear energetic preference is observed for the cleavage of the chemically distinct Lys-Gly, Phe-Phe, and His-Gln bonds, respectively. However, the scissile peptide bond lengths in the corresponding reactants are the same (1.37 Å). The process occurs through the same pathway in the mechanism of PET hydrolysis by **NEP** (Figure 3a). Here, the double proton transfer takes place with a barrier of 9.1 kcal/mol. Here, it is worth mentioning that an ester bond is substantially more susceptible to hydrolysis than a peptide bond. Additinally, **MMP** with the rate-limiting barrier of 17.5 kcal/mol for Phe-Phe hydrolysis is more active than **IDE**.

In the mechanism utilized by **BILAP**, the bicarbonate ion functions as an acid, similar to Glu in mononuclear metallopeptidases, and cleaves the peptide bond through a proton transfer (Figure 3b).[140] This process occurs in the rate-limiting step with a barrier of 25.5 kcal/mol. The bicarbonate ion has been implicated in a similar acid/base role in the proposed mechanism of cyclopropane synthase.[148, 149] The barrier is in line with the experimentally measured barrier of 18.7 kcal/mol.[144] In an alternative pathway, a cluster of three water molecules can play the role of the bicarbonate ion.[150] The barrier for such a pathway is 4.9 kcal/mol higher than the one using the bicarbonate ion as the acid/base residue. However, **SgAP** accomplishes bond cleavage through a process similar

to the one utilized by mononuclear metallopeptidases (Figure 3b). The two-proton transfer process that this enzyme employs is supported by experiments.[124, 146] The overall barrier of 16.5 kcal/mol for the mechanism is in agreement with the measured value of 13.9 kcal/mol.[124] The peptide bond cleavage step is the rate-limiting-step of the mechanism.[145] The measured solvent kinetic isotope effects (KIEs) also suggest that the creation of the nucleophile in the first step and collapse of the *gem*-diolate intermediate in the second step is the rate-determining step at pH = 6.5 and < 8, respectively.[146]

The above-discussed results indicate that binuclear enzymes are more efficient in activating the water molecule to create a hydroxyl nucleophile due to its bridging binding mode. However, the nucleophilicity of the hydroxyl group is lower in this mode.

IIb. Peptide hydrolysis by synthetic analogues. In the section, mechanisms of several mononuclear and binuclear analogues of metallohydrolases are discussed (Figure 4). These complexes are mostly synthesized using non-biological metal ions and missing the effects of catalytic acid/base residue and non-covalent interactions provided by the second coordination shell residues of natural metallohydrolases. Their activities can be switched from residue-selective to sequence-specific by changing the pH. For instance, the cleavage is residue-selective in acidic aqueous solution, while sequence-specific in mildly acidic and neutral solutions.[151] Thus, they are very useful models to understand the roles of metal ions, residue-selectivity and the sequence-specificity in peptide hydrolysis. Additionally, they can be used as hydrolytic agents in modern bioanalytical and bioengineering applications such as protein footprinting, proteomics and bioengineering of fusion proteins.[152-154] A vast majority of currently available enzymes and

synthetic agents are ill-suited for these applications.[155] For instance, enzymes exhibit broad specificities, function under narrow temperature and pH conditions and are expensive. On the other hand, synthetic reagents such as cyanogen bromide are toxic and provide limited selectivity and low yields. They also require harsh conditions and a larger quantity of the starting material. Thus, metal complexes discussed below provide useful insights into the mechanisms of natural enzymes and help with the design of the next generation of analogues. It is noteworthy that they also possess several shortcomings such as a lack of proper metal ion(s), ligand environment, coordination number and second coordination shell residues. None the less, similar to enzymes, such molecules can utilize either a metal bound or a free water molecule for hydrolysis. However, these pathways cannot be readily distinguished by purely kinetic methods.

IIb1. Pd complexes. The $[Pd(H_2O)_4]^{2+}$ ($\mathbf{I_D}$) complex is one of the simplest mimics of mononuclear metallopeptidases (Figure 4). It can hydrolyze the proximal X-Y (Gly-Gly, Gly-Pro, and Gly-Sar) peptide bond (Sar = sarcosine) in X-Y-Met and X-Y-His sequences in weakly acidic aqueous solutions (Figure 2).[156] However, unlike natural enzymes, it anchors Met and His residues, respectively, of the sequences and cleaves all X-Y peptide bonds irrespective of their chemical nature (Figure 5a). Thus, the substrate provide a major portion of the ligand environment. It has been reported to hydrolyze the R-Gly-Pro-Met, R-Gly-Pro-His, R-Gly-Sar-Met and R-Gly-Gly-Met peptide with the measured rate constants 6.0×10^{-2}, 9.4×10^{-2}, 1.4×10^{-2} and 2.8×10^{-3} min^{-1}, respectively, at pH 2.0 and 60 °C that correspond to barriers of 24.0, 23.8, 25.0 and 26.1 kcal/mol respectively.[156] The mechanisms for the cleavage of all four sequences catalyzed by $\mathbf{I_D}$ were investigated using DFT calculations.[157] According to the suggested mechanism, similar to mononuclear enzymes, a Pd bound water is utilized for hydrolysis (Figure 5a). Here, activations

of both the substrate and water molecule by the metal cation and substrate are substantially weaker than in the mononuclear enzymes. A proton transfer from the Pd-bound water to the substrate with the simultaneous nucleophilic attack cleaves the peptide bond (Figure 5a). The computed barriers of 38.3, 41.4, 39.8 and 39.2 kcal/mol for the hydrolysis of the Gly-Pro-Met, Gly-Pro-His, Gly-Sar-Met and Gly-Gly-Met, respectively, are in agreement with the measured rate constants at pH 2.0 and 60 °C.[156] The corresponding barriers using an external water molecule are much higher (> 50.0 kcal/mol) for all four sequences.

A second metal center is included in this complex, $[Pd_2(\mu\text{-}OH)([18]aneN_6)]^{4+}$ (where $[18]aneN_6$ is 1, 4, 7, 10, 13, 16-hexaazacyclooctadecane), $\mathbf{I_{DD}}$], to create a mimic of binuclear hydrolases (Figure 4).[139] In $\mathbf{I_{DD}}$, unlike $\mathbf{I_D}$ and natural enzymes, the Phe-Phe-Met substrate is not coordinated to a metal ion and associates indirectly through hydrogen bonding with the metal bound water. This complex, in contrast to $\mathbf{I_D}$, utilizes an external water molecule trapped between the substrate and the metal-bound water molecule for hydrolysis (Figure 5b). The external water abstracts a proton from the Pd1-coordinated water and forms a hydronium ion $(H_3O)^+$. The subsequent nucleophilic attack to cleave the peptide bond occurs with a barrier of 31.0 kcal/mol. The inclusion of the second metal center lowers the barrier by 4.4 kcal/mol in comparison to mononuclear $\mathbf{I_D}$.[139] Evidently, $\mathbf{I_{DD}}$ employs a much different mechanism than $\mathbf{I_D}$ and natural enzymes. Nonetheless, the effect of the second metal center is similar to the one observed in the hydrolysis of phosphate esters, where binuclear model complexes are found to be more effective than the mononuclear ones.[158-160] However, the barrier for $\mathbf{I_{DD}}$ is still substantially higher than both mono- and binuclear enzymes.

Furthermore, substrate specificity is incorporated in the complex by attaching the hydrophobic moiety of β-cyclodextrin (CD) to create the 6-S-2-(2-mercaptomethyl)-propane-6-deoxy-β-cyclodextrin diaqua palladium(II), $I_{D\text{-}CD}$ complex (Figure 4).[161] In $I_{D\text{-}CD}$, the hydrophobic enzyme like cavity of CD could enhance its activity because low entropy and conformational enthalpy are spend in approaching the transition state.[162] This complex has been reported to sequence-specifically cleave the un-activated tertiary Ser-Pro peptide bond in the sequence Ser-Pro-Phe of the bradykinin substrate at pH 7.0 and 60°C (Figure 2).[161] The hybrid quantum mechanics/molecular mechanics (QM/MM: B3LYP/Amber) calculations show that both the substrate and water molecule are directly coordinated to the Pd ion.[163] Again, Pd-bound water and not a free water is energetically more feasible for hydrolysis, as observed for natural enzymes and I_D. The barrier of the concerted mechanism employed by the complex is 32.8 kcal/mol, which is similar (31.0 kcal/mol) to the one computed for the binuclear I_{DD} complex. The presence of CD increases the nucleophilicity of the hydroxyl group and moves it closer to the electrophile. Its removal from the model increases the barrier by 7.4 kcal/mol. However, this barrier is 9.0 kcal/mol higher than the measured value.[161] It could be partially attributed to the measurement of the rate constants at 60 °C, whereas calculations were performed at 25 °C. Therefore, due to the temperature dependence of the pre-exponential constant in the Arrhenius equation, it is not possible to accurately estimate the measured barrier at 25 °C. However, the optimum location of the CD ring is not clear. Its inclusion of two -CH$_2$ groups downstream from the S atom of the substrate increases its activity by as much as 3×10^5 times. Rather surprisingly, the addition of the second CD ring makes only a small effect on the barrier. It should facilitate a rapid formation of the substrate-catalyst complex and accelerate the rate of reaction. However, in computational models the substrate is already coordinated to the complex. The substitution of Pd with biologically

relevant Zn and Co increases the barrier by 3.1 kcal/mol (35.9 kcal/mol) and decreases by 6.2

kcal/mol (26.6 kcal/mol), respectively.

These results suggest that either the inclusion of the second metal center in ($\mathbf{I_{DD}}$) or the

hydrophobic CD cavity ($\mathbf{I_{D\text{-}CD}}$) enhances the activity of $\mathbf{I_D}$. Their higher barriers can also be

attributed to the cleavage of the hydrolysis resistant tertiary peptide bond formed by a Pro residue.

IIb2. Metal-cyclen complexes. In these complexes a macrocycle ring of 1,4,7,10-

tetraazacyclododecane (cyclen) and 1-oxa-4,7,10-triazacyclododecane (oxacyclen) is coordinated

to a metal ion (Figure 4). For instance, transition metal complexes of cyclen ($\mathbf{I_C}$) and oxacyclen

($\mathbf{I_{OC}}$), where M = Co(III) or Cu(II), have been reported to selectively hydrolyze a wide range of

biomolecules such as lysozyme, albumin, myoglobin, and Aβ peptide.[164-167] Furthermore, the

inclusion of an organic group or an aromatic chain (pendant) provide bond specificity in a manner

different from the CD cavity of $\mathbf{I_{D\text{-}CD}}$ and enzyme active sites.[168] Based on its chemical structure,

the pendant covalently links to a specific chemical group of the substrate and positions the metal

center adjacent to the scissile bond. In the reactants of $\mathbf{Co\text{-}I_C}$ and $\mathbf{Cu\text{-}I_C}$, the hydroxyl nucleophile

is already attached to the metal ion unlike a water molecule in $\mathbf{I_D}$ (Figure 5c).[169] The Cu(II)-

nucleophile bond distance in $\mathbf{Cu\text{-}I_C}$ is 0.07 Å longer than the corresponding distance in the $\mathbf{Co\text{-}I_C}$

case. Additionally, all metal-ligand bond distances for $\mathbf{Cu\text{-}I_C}$ are longer than the ones for $\mathbf{Co\text{-}I_C}$.

However, the Phe-Ala substrate is bound directly only in the latter *i.e.* coordination number of the

Cu(II) and Co(III) ions is 5 and 6, respectively. The scissile peptide bond in $\mathbf{Cu\text{-}I_C}$ is also 0.01 Å

longer than the bond in $\mathbf{Co\text{-}I_C}$. The nucleophilic attack on the substrate occurrs with a barrier of

19.8 and 24.1 kcal/mol for **Cu-I$_C$** and **Co-I$_C$**, respectively (Figure 5c). This difference is attributed

to the provision of a stronger nucleophile in the former. In the next step, a proton transfer from the

nucleophile to the N atom of the substrate leads to its cleavage (Figure 5c). From the respective

intermediates, the barriers for this process are comparable for **Cu-I$_C$ and Co-I$_C$** *i.e.* 19.0 and 19.5

kcal/mol, respectively. The removal of the pendent from **Cu-I$_C$** and **Co-I$_C$** reduces the barrier by

3.0 and 9.3 kcal/mol, respectively. The barrier of 30.5 kcal/mol for the **Co-I$_C$** complex without the

pendent is in agreement with the measured barrier of 25.9 kcal/mol for the hydrolysis of myoglobin

at pH 9.0 and 50°C.[170] Additionally, barriers of 39.8 kcal/mol for **Co-I$_C$** and 40.1 kcal/mol for its

oxacylen derivative **Co-I$_{OC}$** for the same mechanism are supported by the measured data that their

activities differ by only four times.[164] Furthermore, Ni (in the triplet state) is the most feasible

substitution among Ni(II), Zn(II), Cd(II), and Pd(II) complexes without pendent and hydrolyzes

the peptide bond with the lowest barrier of 27.2 kcal/mol.

The results discussed above suggest that the electronic state of the metal ion is critical in the

activities of these complexes. In the mechanisms of **I$_D$** and **I$_C$** only the first step is different *i.e.* the

former created the hydroxyl nucleophile from a water molecule, while it is already present in the

latter. It is found that with the barrier of 33.7 kcal/mol **Cu-I$_C$** is more active than **Co-I$_C$** and **I$_D$** that

hydrolyzes the dipeptides with the barriers of 38-42 kcal/mol.

IIb3. Zr-azacrownether Complexes: To specifically study the effects of the coordination number

of the metal ion and charge of the ligand on the hydrolysis of the Gly-Gly (neutral) dipeptide

(Figure 2), activities of 11 different N$_2$O$_4$, N$_2$O$_3$, and NO$_2$ core containing mononuclear Zr(IV)

complexes (**I$_A$**), 4,13-diaza-18-crown-6 (**I$_{A-N2O4}$**), 1,4,10-trioxa-7,13-diazacyclopentadecane (**I$_{A-}$**

$_{N2O3}$) and 2-(2-methoxy)-ethanol ($\mathbf{I_{A\text{-}NO2}}$), respectively, and their analogues have been investigated (Figure 4).[171] Additionally, the effect of the charge of the substrate is investigated using Gly-Glu (negative) and Gly-Lys (positive) as the substrates. Due to the high coordination number of Zr(IV), the metal ion provide binding sites to the Gly-Gly substrate and hydroxide nucleophile.

Based on the experimental information, the protonation states (singly protonated, doubly protonated or doubly deprotonated) and number of ligands were altered (Figure 4). They all exist in the hepta-coordinated state and both substrate and hydroxyl nucleophile are directly coordinated to the Zr(IV) ion (Figure 6a). Among the complexes with the N_2O_4 ligand, double deprotonation of the nitrogen atoms in $\mathbf{I_{A\text{-}DN2O4}}$ elongates the most metal – ligand distances and increases the Lewis acidity of the metal ion.[171] The longest metal-nucleophile distance in the complex is also indicative of a stronger nucleophile.[172] These factors render $\mathbf{I_{A\text{-}DN2O4}}$ as the most active complex in this ligand environment. In $\mathbf{I_{A\text{-}DN2O4}}$, the nucleophile attack on the substrate occurs with a barrier of 13.9 kcal/mol (Figure 6a). The single and double protonation of ligands increase the barrier by 6-12 kcal/mol. It is apparently caused by a decrease in the nucleophilicity of the hydroxyl ion. The intermediate formed in this process is endothermic by 13.6 kcal/mol. It becomes more unstable by 7-23.0 kcal/mol upon the single and double protonation of the ligands. The overall barrier of the mechanism increases by 10.0 - 17.0 kcal/mol in the protonated complexes and becomes comparable to the barriers of $\mathbf{Co\text{-}I_{MC}}$ and $\mathbf{I_D}$ complexes.[169] On the other hand, the deprotonated form of a smaller NO_2 core with two hydroxyl ligands ($\mathbf{I_{A\text{-}DNO2\text{-}2H}}$) creates the most active form among all 11 complexes (Figure 4). In $\mathbf{I_{A\text{-}DNO2\text{-}2H}}$, the Zr(IV) is bound to the substrate, nucleophile and two additional hydroxyl groups. In the complex, the Zr-substrate and Zr-nucleophile distances are the longest and the peptide bond is most activated. Consequently, it is the most active complex

with the lowest barrier (28.9 kcal/mol). In comparison to the Gly-Gly substrate, the barrier for the Gly-Glu and Gly-Lys dipeptides is reduced by 1.4 kcal/mol and increased by 3.1 kcal/mol, respectively. Similar to **IDE**, this simple complex also exhibits substrate preference. These results are supported by the measured level of hydrolysis for the substrates i.e. Gly-Glu, pH 7.2, 60 °C, 20 h, yield 97% > Gly-Gly, pH 7.0, 60 °C, 20 h, yield 90% > Gly-Lys, pH 7.1, 60 °C, 20 h, yield 17%.[173]

These results show that among the two competing effects, Lewis acidity and nucleophile activation, the latter dominates the activities of the complexes.

IIb4. Zr-Polyoxometalates. Zr(IV)-substituted polyoxometalates (Zr-POMs, **I$_P$** in Figure 4) are chemically more complex than the previous mononuclear metal complexes (**I$_D$**, **I$_C$** and **I$_A$**). They are metal-oxygen clusters that also hydrolyze multiple peptide bonds of many critical molecules such as human serum albumin (HSA), hen egg-white lysozyme (HEWL), myoglobin, insulin chain B and cytochrome c.[174-178] The monomeric 1:1 Zr(IV) Keggin POM (**I$_P$**) has been reported to catalyze the hydrolysis of four distinct peptide bonds [Arg-Leu (site 1), Ala-Asp (site 2), Lys-Asp (site 3) and Cys-Glu (site 4)] of HSA (Figure 2) at pH 7.4 and 60 °C.[178] Its lack of selectivity is similar to mononuclear peptidases that are also known to hydrolyze different peptide bonds of their substrates. **I$_P$** and drug molecules such as ibuprofen and diazepam have been proposed to predominantly interact at the site 4 - known as Sudlow's drug site II (Figure 2).[179, 180,181, 182] The structures of the **I$_P$-HSA** complexes were built using molecular docking and MD simulations.[183] The binding free energy for this site computed using the lambda (λ) particle approach [184-186] is found to be the most favorable (-21.8 kcal/mol) among the four binding sites.

 The mechanism of HSA hydrolysis by $\mathbf{I_P}$ was investigated using the two-layer QM/MM ONIOM method utilizing the previous MD equilibrated structures (Figure 6b).[187] In the reactant, similar to other complexes, the hydroxyl nucleophile is already coordinated to the Zr(IV) ion but unlike natural enzymes, there is no direct metal-substrate coordination. The substrate interacted indirectly through two hydrogen bonds with the metal-bound hydroxyl group. These interactions suggest that Lewis acidity of the Zr ion is not critical. The generation of tetrahedral intermediate through the attack by the metal-coordinated hydroxyl group occurrs with a barrier of 18.3 kcal/mol. This process is endothermic by 8.0 kcal/mol. The barrier for the process using an external water molecule is higher by 4.1 kcal/mol. In the next rate-limiting step, the cleavage of the peptide bond through proton transfer from the nucleophile occurs with an overall barrier of 27.5 kcal/mol. The high strain of a four-membered ring in the step contributes to its high energy barrier. This process is quite different in natural enzymes, where a base/acid residue facilitates the bond cleavage. The barrier, although significantly higher than natural metallohydrolases, is comparable to the measured values of 24.6-27.0 kcal/mol at pD 5.4 and 60 °C for the hydrolysis of 18 different dipeptides by its dimeric form.[188] Additionally, it is comparable to most active forms of $\mathbf{I_{D\text{-}CD}}$ (Co-variant) and $\mathbf{I_C}$ (Ni-variant) with the barriers of 26.6 and 27.2 kcal/mol, respectively. Furthermore, the computed barrier for the peptide bond cleavage is 36.0, 31.0, 35.5 and 27.5 kcal/mol for the [Arg-Leu (site 1), Ala-Asp(site 2), Lys-Asp(site 3) and Cys-Glu (site 4)] sites, respectively and exhibits the clear energetic preference for their hydrolysis.

Our results indicate that the Lewis acidity of the Zr ion and nucleophilicity of the hydroxyl ions are different for these cleavage sites. This site preference is similar to **IDE** albeit several orders of magnitude slower due to the lack of acid/base residue and protein surrounding.

IIc. Phosphoester Hydrolysis: Glycerophosphodiesterase (**GpdQ**) from *Enterobacter aerogenes*[189, 190] exhibits extensive substrate promiscuity (Figure 1). It is predominantly a diesterase but hydrolyzes a range of non-natural phosphomono-, phosphodi- and phosphotriester substrates such as 4-nitrophenyl phosphate (NPP), glycerol-3-phosphoetanolamine (GPE), bis(4-nitrophenyl) phosphate (BNPP), diethyl 4-nitrophenyl phosphate (paraoxon) and several organophosphate pesticides and nerve agents such as paraoxon, demeton, sarin, soman and VX (Figure 2).[74, 75, 189-192] Consequently, it could be used in agricultural remediation and as an anti-warfare agent.[73-75, 193] This enzyme creates its catalytically active binuclear $Fe(N_2O_2)$-$Zn(N_2O_2)$ [Fe(His, His, Asp, Asp)-Zn(His, His, Asp, Asn)] core only in the presence of the substrate (Figure 1).[192, 194-197] After its generation, **GpdQ** utilizes its remarkable coordination flexibility, also known as "breathing of the active site cleft" to hydrolyze diverse substrates with different sizes and chemical compositions. On the other hand, as discussed above, the $Zn1(NO_2)$-$Zn2(NO_2)$ core containing **SgAP** (Figure 1) is also capable of accelerating the first-order hydrolysis of the phosphodiester bis(4-nitrophenyl) phosphate (BNPP), (Figure 2), by 10^{10}-fold in comparison to the uncatalyzed reaction.[123, 198] This is one of the rare examples in which an aminopeptidase hydrolyzes its transition-state analogue, a phosphoester, at an enormous rate.

The phosphoester hydrolysis can occur through three distinct mechanisms shown in the More O'Ferrall–Jencks diagram (Figure 7).[199] (a) Dissociative or elimination-addition mechanism: It involves the formation of a trigonal metaphosphate intermediate and release of the leaving group

(R_1O) precedes the formation the phosphate-nucleophile (P^+-OH^-) bond (Figure 7a). (b) Dissociative- associative or synchronous mechanism: It occurs through the concomitant formation and cleavage of the phosphoester bonds (S_N2 type mechanism in Figure 7b). (c) Associative or addition-elimination mechanism: This mechanism involves the formation of a pentavalent phosphorane intermediate by the nucleophile attack (Figure 7c). In general, binuclear metallohydrolases have been reported to utilize one of these mechanisms depending on the chemical nature of the substrate.[12, 200-209] However, the dissociative mechanism has not been observed for such substrates. Since the associative mechanism has been found to be energetically most feasible mechanism,[145, 210] the activities of both **GpdQ** and **SgAP** are discussed using only this mechanism for BNPP hydrolysis (Figure 1 and 2).

IIc1. Creation of the phosphorane intermediate. In the reactant of **GpdQ**, one of the nitrophenyl groups directly interacts with the active site, while the second group is exposed to the solvent.[211] In this structure, the scissile P-O bond of BNPP is significantly elongated by 0.10 Å in comparison to its free form due to double Lewis acid activation.[210] The nucleophile generating water is also directly coordinated to the Fe ion (M1 in Figure 7). These interactions lower its pK_a value significantly and increase its acidity (O-H = 1.02 Å). This strategy has also been utilized by other binuclear phosphoesterases like *E.coli* alkaline phosphatase[208] and OpdA[202]. The pK_a of the water molecule for **GpdQ** is measured to be ~9.5.[192] In the mechanism, a proton transfer from the Fe-bound water through a chain of three water molecules to His-Asp dyad creates the hydroxyl nucleophile.[210] A histidine residue has been proposed a similar role in the mechanisms of PAP,[212] RNaseZ[213] and phosphoprotein phosphatases.[214] Due to the high acidity of the water molecule and basicity of the dyad, this process occurs through a very low barrier of 1.9 kcal/mol and form an

intermediate that is endergonic by only 0.6 kcal/mol. In the intermediate, phosphorane species is not created and the hydroxyl nucleophile is still bound to the Fe ion (Figure 7c).

However, in comparison to **GpdQ**, among the two almost equivalent metal sites (site 1 or 2) in **SgAP**, the actual location of the nucleophile generation is not known (Figure 1).[145] Here, the generation of the nucleophile at site 2 is found to be slightly more favorable by 1.8 kcal/mol. In the reactant, in comparison to monodentate binding to Zn in **GpdQ**, BNPP coordinate in an asymmetric bridging mode to both metals but through a much shorter bond with Zn1. In this binding mode, similar to **GpdQ**, the scissile O-P bond of BNPP gets activated by 0.08 Å than the corresponding bond in its free form due to double Lewis acid activation. However, the activation is lower than the one (0.10 Å) observed for **GpdQ**. The nucleophile generating water in **SgAP** is more activated (O-H = 1.03 Å) than in the **GpdQ** case. In the first step of the mechanism employed by **SgAP**, in contrast to the mechanism utilized by **GpdQ**, abstraction of a proton from the Zn2 bound water by the Glu base occurs synchronously with the nucleophilic attack to BNPP (Figure 7). The barrier for the concerted process is 16.8 kcal/mol. It is in excellent agreement with the measured value of 18.3 kcal/mol.[124] For **GpdQ**, the barrier for such a concerted pathway is significantly higher by ~10.0 kcal/mol.[210] In the intermediate, the nucleophile is attached to the substrate. Here, the P-O bond is significantly activated by 0.21 Å and stabilized through hydrogen bonding by two second coordination shell residues. It is endergonic by 3.6 kcal/mol, whereas this process is almost thermoneutral in **GpdQ**.

IIc2. Cleavage of the phosphodiester bond. As noticed in the first step, **GpdQ** and **SgAP** utilize different pathways for the cleavage of the scissile P-O bond (Figure 7). In **GpdQ**, an in-line

(associative-dissociative) nucleophilic attack by the Fe-bound hydroxyl group cleaves the P-O bond. The process crosses overs a barrier of 10.1 kcal/mol in this rate-determining step. In the final product, negatively charged *p*-nitrophenolate and *p*-nitrophenyl phosphate fragments are formed. However, in **SgAP** donation of a proton by the neutral Glu to the leaving group of BNPP, instead of a nucleophile attack in **GpdQ**, cleaves the P-O bond. It takes place with a small barrier of 5.7 kcal/mol and the same *p*-nitrophenol and *p*-nitrophenyl phosphate fragments are formed. They are bound in the same fashion as the phosphate ion in the crystal structure.[215]

These results show that the heterobinuclear **GpdQ** and homobinuclear **SgAP** utilize distinct mechanisms for BNPP hydrolysis. **GpdQ** bypasses the formation of the phosphorene intermediate and uses the S_N2 type associative-dissociative mechanism. However, **SgAP** utilizes the associative mechanism that involves the generation of the phosphorane intermediate. Additionally, the cleavage of the P-O bond is the rate-determining process for **GpdQ**, while the generation of the nucleophile for **SgAP**. Furthermore, **GpdQ** catalyzes this reaction with 6.7 kcal/mol lower barrier than the barrier computed for **SgAP**. Our results are in line with experimental observations that in general heterobinuclear centers are more active than their homobinuclear counterparts for hydrolysis.[27] Since **SgAP** catalyzes both peptide and phosphoester hydrolysis, it provides a unique opportunity to compare controlling factors of these reactions. For instance, the first step of BNPP hydrolysis is dominated by its double Lewis acid activation, while for Leu-*p*NA hydrolysis by stronger nucleophilicity of the metal bound hydroxyl group. In general, they are competing effects and the two reactions catalyzed by *Sg*AP provide an ideal system to study their influences. Furthermore, in contrast to the second step in the Leu-*p*NA hydrolysis, the nucleophile generation

is the rate-limiting step for the BNPP hydrolysis. These results suggest that the chemical nature of the substrate influences energetics of the nucleophile generation and its attack on the electrophile.

IId. Synthetic Analogues.

IId1. Metal-cyclen complexes. The cyclen group containing complexes of divalent Zn and Cu (**Zn-I$_C$** and **Cu-I$_C$**) have also been reported to hydrolyze the phosphoester bond of BNPP and supercoiled DNA, respectively (Figure 2 and 4).[216,217] Additionally, several cyclen ring possessing complexes of tri- and tetravalent lanthanides (Eu, La, Zr and Ce) have also been used for this reaction.[218-222] Therefore, BNPP hydrolysis by **I$_C$** is investigated using two types of metal ions, divalent [Zn(II), Cu(II) and Co(II)] and tetravalent [Ce(IV), Zr(IV) and Ti(IV)].[223] In the energetically most feasible mechanism for the divalent metal-cyclen complexes, BNPP interacts with the metal ion in a monodentate mode and due to its Lewis acidity the metal ion activates the scissile phosphoester bond by ~0.04 Å.[223] The hydroxyl nucleophile is also bound to the metal ion. Its attack on the phosphorus center of BNPP generates a five-membered trigonal bipyramidal phosphorane intermediate (Figure 8a). This process occurs with a barrier of 20.7 kcal/mol and the intermediate is endergonic by 15.5 kcal/mol. In the intermediate, the scissile P-OR bond *trans* to the nucleophile is substantially elongated but not completely broken. In the next barrierless step, the intermediate collapses through the cleavage of the P-OR bond. The barriers of 22.0 and 23.4 kcal/mol for **Cu(II)-I$_C$** and **Co(II)-I$_C$**, respectively, are slightly higher than the barrier (20.7 kcal/mol) for **Zn-I$_C$**. This difference is caused by the provision of a stronger nucleophile by the **Zn-I$_C$**. Thus, both Lewis acidity and nucleophilicity of the metal center are critical in the activities of these complexes.

Due to high coordination numbers (6-12) of tetravalent (Ce, Zr and Ti) metals, BNPP coordinates in a bidentate manner in their complexes. In contrast to Lewis acid activation of BNPP in the complexes of divalent ions, here the P-O bond actually becomes stronger by ~0.03 Å. The barriers (> 30 kcal/mol) for all tetravalent metal complexes are substantially higher than their divalent counterparts. In comparison to the divalent metals, the lower activity of the complexes with different coordination numbers (7-9) is caused by the strengthening of the scissile phosphoester bond and weakening of the nucleophilicity of the hydroxyl nucleophile.

A comparison of peptide (29.7-31.9 kcal/mol) and phosphoester (20.7-23.4 kcal/mol) hydrolysis reveals that I_C is a more efficient phosphoesterase with divalent metals. That is due to the higher Lewis acidity of the metal ion in phosphoester hydrolysis.

IId2. Hetero- and homobinuclear complexes. The heterobinuclear asymmetric Fe^{III}-Zn^{II} core containing complex $[I_B(OH)Fe^{III}(\mu\text{-}OH)Zn^{II}]^+$ (**FZ-I_B**), where I_B (bpbpmp) = 2-bis[{(2-pyridylmethyl)-aminomethyl}-6-{(2-hydroxybenzyl)-(2-pydidylmethyl)}-aminomethyl]-4-methylphenol), contains catalytically active $[(OH)Fe^{III}(\mu\text{-}OH)Zn^{II}(OH_2)]^+$ species in aqueous solution (Figure 4).[224] This complex is a true mimic of metallohydrolases and increases the rate for hydrolysis of bis(2,4-dinitrophenyl) phosphate (BDNPP) by 4.8×10^3-fold ($k_{cat} = 9.13 \times 10^{-4}$ s^{-1}) at pH 6.5 (Figure 2). In contrast, a homobinuclear Cu^{II}-Cu^{II} core-possessing symmetric complex $[II_BCu^{II}(\mu\text{-}OH)Cu^{II}]^{2+}$ (**CC-II_B**), where II_B (bcmp) = 2,6-bis(1,4,7-triazacyclonon-1-ylmethyl)-4-methylphenol), hydrolyzes BDNPP with a second order rate constant of 0.047 $M^{-1}.s^{-1}$ at pH 8.0 and 40 °C (Figure 4).[24, 225] **CC-II_B** is also able to hydrolyze DNA and induces cell death in pancreatic cancer cells. Its Zn variant (**ZZ-II_B**) also hydrolyzes BDNPP with an apparent second

order rate constant of 0.028 $M^{-1}.s^{-1}$ under the same conditions (Figure 4).[226] In the reactant of **FZ-I$_B$**, both Fe^{III} and Zn^{II} ions are coordinated to 6 ligands in a distorted octahedral coordination environment (Figure 8b).[227] Here, Fe^{III} is located in the N_2O_2 site and Zn^{II} in the N_3O site. BDNPP is coordinated to the Zn^{II} ion in a monodentate fashion that is supported by experimental data.[224] However, as noticed above for other metal complexes, no Lewis acid activation of the substrate is observed and the catalyst-substrate interaction actually strengthens the scissile P-O bond by 0.04 Å in comparison to the corresponding bond in its free form.[227] That is in contrast to the activation of the scissile P-O bond of BNPP in the mechanisms utilized by **GpdQ**[210] and **SgAP**[145]. In an S_N2-type reaction an in-line concerted attack of the Fe^{III} bound hydroxyl nucleophile of **FZ-I$_B$** on the electrophilic P atom of BDNPP leads to the cleavage of the scissile P-O bond with a barrier of 15.8 kcal/mol. It is in good agreement with the measured barrier of 20.1 kcal/mol.[224] It is, however, 5.7 kcal/mol higher than the corresponding barrier computed for **GpdQ**,[210] demonstrating that **FZ-I$_B$**, formed by organic ligands, is substantially less active than natural enzymes. In contrast to the use of double Lewis acid activation by the binuclear metal cores of natural hydrolases, this mechanism is dominated by the nucleophilicity of the Fe^{III}-coordinated hydroxyl group.

In contrast to **FZ-I$_B$**, BDNPP in di-zinc core containing **ZZ-I$_B$** interacts through a strong hydrogen bond with the μ-OH group and π-π interactions with the ligand of Zn1. In **ZZ-I$_B$**, the computed barrier for the cleavage of the P-O bond through the attack by the -OH nucleophile is only 6.3 kcal/mol, which is 9.5 kcal/mol lower than the barrier in **FZ-I$_B$**. Due to the low ligand field stabilization energy of the Zn ion, both metal-nucleophile distances in **ZZ-I$_B$** are substantially longer than the Fe-O distance in **FZ-I$_B$**. The reason for the significantly lower barrier in **ZZ-I$_B$** when compared to **FZ-I$_B$** is the provision of a stronger nucleophile in the former. Similar to **ZZ-**

I_B, BDNPP does not bind directly to the metal ions in the dicopper core-possessing CC-I_B (coordination numbers are 5 and 6 for Cu1 and Cu2, respectively). However, the substrate binding mode is quite different in the two systems. In this structure, the hydroxyl group is terminally bound to the Cu2 atom. Despite the lack of a direct bond between the metal and substrate, rather surprisingly, the P-O bond in CC-I_B is 0.03 Å longer than in FZ-I_B due to Lewis acid activation. For CC-I_B, the barrier for the cleavage of the P-O bond is 11.4 kcal/mol, 4.4 lower and 5.1 kcal/mol higher than the corresponding barrier for FZ-I_B and ZZ-I_B, respectively.

The above results demonstrate that the ligand environments and substrate binding modes of the three distinct metal clusters in the same ligand environment are different. In the absence of a Lewis acid activation the energetics of this process are dominated by the nucleophilicity of the hydroxyl ion. The identities of the metal ions determine the activities of their complexes, and ZZ-I_B is found to be the most active complex. Overall, complexes formed with the asymmetric ligand I are more reactive than their symmetric counterparts formed by ligand II. The terminal hydroxyl group is a stronger nucleophile than its bridging counterpart. An electron donating group (-CH_3) at the para position of the centered phenolate group of the ligand increases the nucleophilicity of the hydroxyl group.

III. Summary and Outlook. The design of efficient synthetic metallohydrolases has been widely acknowledged as a formidable task. It is not surprising that in comparison to natural enzymes, hydrolytic reactions promoted by the existing metal complexes are substantially slower and occur with lower catalytic turnover. It could be due to the following reasons: (1) the absence of chemical properties of amino acid residues of enzyme active sites; (2) they contain one to three more ligands

than the metal centers of enzymes; (3) the lack of combined influence of non-covalent interactions; and (4) the absence of second coordination shell residues of enzymes. The design of analogues with improved activities requires a deep understanding of the roles of metal ions, ligands (direct and indirect) and the environment in the functioning of natural and synthetic metallohydrolases and chemical modifications in the latter on the basis of those insights. However, realization of this goal is very challenging and requires a rigorous integration of experiments and theoretical calculations. The experimental mechanistic studies on natural enzymes are hindered by extremely fast rates of reactions, a lack of substrate bound structures, kinetic indistinguishability of pathways, inhibition of enzymatic activities upon metal and ligand substitutions and the silence of the diamagnetic metal centers to NMR, electronic, and ESR spectroscopies. On the other hand, despite the availability of considerable experimental data, the mechanistic and structural information regarding the activities of synthetic analogues and chemical alterations for their improvement are not consistently available. However, the current experimental information concerning both natural and synthetic metallohydrolases provides an ideal platform to employ theoretical and computational chemistry techniques to understand the "design" principles and to develop the next generation of synthetic analogues for these critical reactions.

Our computational studies are useful in either addressing or reconfirming the multiple issues regarding metallohydrolases [mono-(**IDE**, **NEP** and **MMP**) and binuclear (**BILAP** and *Sg*AP) metalloproteases and non-enzymatic (I_D, I_C, I_A and I_P) systems for peptide hydrolysis and binuclear (**GpdQ** and *Sg*AP) and non-enzymatic (I_C, I_B and II_B) systems for phosphoester hydrolysis]. For the enzymatic systems the following issues are addressed: (1) A low basicity of the ligand environment in enzymes such as **MMP** enhances the Lewis acidity of the metal ion and

promote hydrolysis; (2) A metal bound water is more suitable than a free water for the creation of hydroxyl nucleophile; (3) The water is more acidic in the bridging than the terminal form in binuclear enzymes; (4) The electronic nature of the metal and substrate predominantly controls the energetics of hydrolysis; (5) The different metal centers such as hetero- and homobinuclear in **GpdQ** and *Sg***AP**, respectively utilize distinct mechanisms for the hydrolysis of the same BNPP substrate; (6) Heterobinuclear metal centers are generally more reactive than their homobinuclear counterparts; (7) Peptide hydrolysis is controlled by the nucleophilicity of the metal bound hydroxyl group, whereas phosphoester hydrolysis by double Lewis acid activation. For the non-enzymatic systems the following issues are addressed: (1) The inclusion of the second metal center (I_{DD}) and hydrophobic cavity of CD (I_{D-CD}) exert similar effects in I_D complexes; (2) The electronic nature of the metal ion is critical in controlling the hydrolytic activities of metal complexes; (3) Among Lewis acidity and nucleophile activation, the latter dominates the activities of metal complexes; (4) The mode of substrate binding influences the nucleophilicity of the hydroxyl ion; (5) The terminal hydroxyl group is a stronger nucleophile than its bridging counterpart; (7) Due to low ligand field stabilization energy, the biologically relevant divalent metal ions such as Zn, Cu and Co are more suitable for hydrolysis.

Quite clearly, these impressive metal complexes can hydrolyze extremely stable bonds at good rates. They were synthesized under diverse conditions and their activities were measured using distinct substrates. In this aspect, our results elucidating the effects of the metal ions, ligands, metal cooperativity, non-covalent interactions, Lewis acidity and nucleophilicity in hydrolysis will be helpful in designing the next generation of synthetic analogues. Although the existing computational techniques can provide useful mechanistic insights utilizing experimental data, they

still cannot make accurate predictions in cases where such information is unavailable. Their success as predictive tool will depend on accurate computations of different chemical factors such as electronic, entropic, solvent and dynamical effects.[228-230]

IV. Authors Contributions. L. S., V. J-Y., L. W. wrote the first draft of the manuscript and P. R., J. Y., S. M. and R. P. revised the manuscript.

V. Conflict of interest.

The authors declare no conflict of interest.

V. References.

1.   B. Zhang and R. Breslow, *J. Am. Chem. Soc.*, 1997, **119**, 1676-1681.

2.   J. Kuwabara, C. L. Stern and C. A. Mirkin, *J. Am. Chem. Soc.*, 2007, **129**, 10074-10075.

3.   A. J. Kirby, *Angew. Chem. Int. Ed. Engl.*, 1996, **35**, 706-724.

4.   M. J. Wiester, P. A. Ulmann and C. A. Mirkin, *Angew. Chem. Int. Ed.*, 2011, **50**, 114-137.

5.   J. Meeuwissen and J. N. H. Reek, *Nat. Chem.*, 2010, **2**, 615-621.

6.   F. Schwizer, Y. Okamoto, T. Heinisch, Y. Gu, M. M. Pellizzoni, V. Lebrun, R. Reuter, V. Kohler, J. C. Lewis and T. R. Ward, *Chem. Rev.*, 2018, **118**, 142-231.

7.   T. Zhang, M. Ozbil, A. Barman, T. J. Paul, R. P. Bora and R. Prabhakar, *Acc. Chem. Res.*, 2015, **48**, 192-200.

8.   A. J. Bard, G. M. Whitesides, R. N. Zare and F. W. McLafferty, *Acc. Chem. Res.*, 1995, **28**, 91-91.

9.   D. E. Wilcox, *Chem. Rev.*, 1996, **96**, 2435-2458.

10.   A. B. Sorokin, *Coord. Chem. Rev.*, 2019, **389**, 141-160.

11.   L. Zhu, O. dos Santos, C. W. Koo, M. Rybstein, L. Pape and J. W. Canary, *Inorg. Chem.*, 2003, **42**, 7912-7920.

12.   G. Schenk, N. Mitić, L. R. Gahan, D. L. Ollis, R. P. McGeary and L. W. Guddat, *Acc. Chem. Res.*, 2012, **45**, 1593-1603.

13.   K. G. Ragunathan and H.-J. Schneider, *Angew. Chem. Int. Ed. Engl.*, 1996, **35**, 1219-1221.

14.   N. Mitić, S. J. Smith, A. Neves, L. W. Guddat, L. R. Gahan and G. Schenk, *Chem. Rev.*, 2006, **106**, 3338-3363.

15.   D. C. Powers and T. Ritter, *Acc. Chem. Res.*, 2012, **45**, 840-850.

16.   H. F. Yuen and T. J. Marks, *Organometallics*, 2008, **27**, 155-158.

17.   K. C. Gupta and A. K. Sutar, *Coord. Chem. Rev.*, 2008, **252**, 1420-1450.

18.   E. Tkatchouk, N. P. Mankad, D. Benitez, W. A. Goddard and F. D. Toste, *J. Am. Chem. Soc.*, 2011, **133**, 14293-14300.

19.   S. Sinha and L. M. Mirica, *ACS Catal.*, 2021, **11**, 5202-5211.

20.   W. Sinha, A. Mahammed, N. Fridman and Z. Gross, *ACS Catal.*, 2020, **10**, 3764-3772.

21.   M. Klähn and M. V. Garland, *ACS Catal.*, 2015, **5**, 2301-2316.

22.   D. G. H. Hetterscheid, S. H. Chikkali, B. de Bruin and J. N. H. Reek, *ChemCatChem*, 2013, **5**, 2785-2793.

23.   D. R. Pye and N. P. Mankad, *Chem. Sci.*, 2017, **8**, 1705-1718.

24.   A. Erxleben, *Coord. Chem. Rev.*, 2018, **360**, 92-121.

25.   B. Das, H. Daver, A. Singh, R. Singh, M. Haukka, S. Demeshko, F. Meyer, G. Lisensky, M. Jarenmark, F. Himo and E. Nordlander, *Eur. J. Inorg. Chem.*, 2014, **2014**, 2204-2212.

26.   S. J. Smith, R. A. Peralta, R. Jovito, A. Horn, A. J. Bortoluzzi, C. J. Noble, G. R. Hanson, R. Stranger, V. Jayaratne, G. Cavigliasso, L. R. Gahan, G. Schenk, O. R. Nascimento, A. Cavalett, T. Bortolotto, G. Razzera, H. Terenzi, A. Neves and M. J. Riley, *Inorg. Chem.*, 2012, **51**, 2065-2078.

27.   M. Jarenmark, S. Kappen, M. Haukka and E. Nordlander, *Dalton Trans.*, 2008, 993-996.

28. F. Nastri, M. Chino, O. Maglio, A. Bhagi-Damodaran, Y. Lu and A. Lombardi, *Chem. Soc. Rev.*, 2016, **45**, 5020-5054.

29. A. E. Tolbert, C. S. Ervin, L. Ruckthong, T. J. Paul, V. M. Jayasinghe-Arachchige, K. P. Neupane, J. A. Stuckey, R. Prabhakar and V. L. Pecoraro, *Nat. Chem.*, 2020, **12**, 405-411.

30. Q. Hu, V. M. Jayasinghe-Arachchige, G. Sharma, L. F. Serafim, T. J. Paul and R. Prabhakar, *WIREs Comput. Mol. Sci.*, 2020, **10**, e1466.

31. X.-P. Zhang, A. Chandra, Y.-M. Lee, R. Cao, K. Ray and W. Nam, *Chem. Soc. Rev.*, 2021, **50**, 4804-4811.

32. S. Kal, S. Xu and L. Que Jr, *Angew. Chem. Int. Ed.*, 2020, **59**, 7332-7349.

33. A. I. Nguyen, R. K. Spencer, Christopher L. Anderson and R. N. Zuckermann, *Chem. Sci.*, 2018, **9**, 8806-8813.

34. A. S. Borovik, *Chem. Soc. Rev.*, 2011, **40**, 1870-1874.

35. S. A. Cook and A. S. Borovik, *Acc. Chem. Res.*, 2015, **48**, 2407-2414.

36. C. Herrero, A. Quaranta, M. Sircoglou, K. Sénéchal-David, A. Baron, I. M. Marín, C. Buron, J.-P. Baltaze, W. Leibl, A. Aukauloo and F. Banse, *Chem. Sci.*, 2015, **6**, 2323-2327.

37. V. A. Larson, B. Battistella, K. Ray, N. Lehnert and W. Nam, *Nat. Rev. Chem.*, 2020, **4**, 404-419.

38. M. Oszajca, M. Brindell, Ł. Orzeł, J. M. Dąbrowski, K. Śpiewak, P. Łabuz, M. Pacia, A. Stochel-Gaudyn, W. Macyk, R. van Eldik and G. Stochel, *Coord. Chem. Rev.*, 2016, **327-328**, 143-165.

39. N. H. Williams, B. Takasaki, M. Wall and J. Chin, *Acc. Chem. Res.*, 1999, **32**, 485-493.

40. W. T. Lowther and B. W. Matthews, *Chem. Rev.*, 2002, **102**, 4581-4608.

41. N. H. Williams and J. Chin, *Chem. Comm.*, 1996, 131-132.

42. J. Qian, W. Gu, H. Liu, F. Gao, L. Feng, S. Yan, D. Liao and P. Cheng, *Dalton Trans.*, 2007, 1060-1066.

43. T. Joshi, B. Graham and L. Spiccia, *Acc. Chem. Res.*, 2015, **48**, 2366-2379.

44. A. Erxleben, *Front. Chem.*, 2019, **7**.

45. C. Piovezan, R. Jovito, A. J. Bortoluzzi, H. Terenzi, F. L. Fischer, P. C. Severino, C. T. Pich, G. G. Azzolini, R. A. Peralta, L. M. Rossi and A. Neves, *Inorg. Chem.*, 2010, **49**, 2580-2582.

46. G. A. d. S. Silva, A. L. Amorim, B. d. Souza, P. Gabriel, H. Terenzi, E. Nordlander, A. Neves and R. A. Peralta, *Dalton Trans.*, 2017, **46**, 11380-11394.

47. Z. Lengyel, C. M. Rufo, Y. S. Moroz, O. V. Makhlynets and I. V. Korendovych, *ACS Catal.*, 2018, **8**, 59-62.

48. F. Yu, V. M. Cangelosi, M. L. Zastrow, M. Tegoni, J. S. Plegaria, A. G. Tebo, C. S. Mocny, L. Ruckthong, H. Qayyum and V. L. Pecoraro, *Chem. Rev.*, 2014, **114**, 3495-3578.

49. A. S. Borovik, *Acc. Chem. Res.*, 2005, **38**, 54-61.

50. G. Mukherjee, J. K. Satpathy, U. K. Bagha, M. Q. E. Mubarak, C. V. Sastri and S. P. de Visser, *ACS Catal.*, 2021, **11**, 9761-9797.

51. P. V. Bernhardt, S. Bosch, P. Comba, L. R. Gahan, G. R. Hanson, V. Mereacre, C. J. Noble, A. K. Powell, G. Schenk and H. Wadepohl, *Inorg. Chem.*, 2015, **54**, 7249-7263.

52. M. Zhao, H.-B. Wang, L.-N. Ji and Z.-W. Mao, *Chem. Soc. Rev.*, 2013, **42**, 8360-8375.

53.   W. Li, F. Li, H. Yang, X. Wu, P. Zhang, Y. Shan and L. Sun, *Nat. Commun.*, 2019, **10**, 5074.

54.   M. Raynal, P. Ballester, A. Vidal-Ferran and P. W. N. M. van Leeuwen, *Chem. Soc. Rev.*, 2014, **43**, 1734-1787.

55.   H. Xu, W. Cao and X. Zhang, *Acc. Chem. Res.*, 2013, **46**, 1647-1658.

56.   Z. Dong, Q. Luo and J. Liu, *Chem. Soc. Rev.*, 2012, **41**, 7890-7908.

57.   Y. Lin, J. Ren and X. Qu, *Acc. Chem. Res.*, 2014, **47**, 1097-1105.

58.   D.-A. Silva, S. Yu, U. Y. Ulge, J. B. Spangler, K. M. Jude, C. Labão-Almeida, L. R. Ali, A. Quijano-Rubio, M. Ruterbusch, I. Leung, T. Biary, S. J. Crowley, E. Marcos, C. D. Walkey, B. D. Weitzner, F. Pardo-Avila, J. Castellanos, L. Carter, L. Stewart, S. R. Riddell, M. Pepper, G. J. L. Bernardes, M. Dougan, K. C. Garcia and D. Baker, *Nature*, 2019, **565**, 186-191.

59.   Y. Lu, N. Yeung, N. Sieracki and N. M. Marshall, *Nature*, 2009, **460**, 855-862.

60.   H. Wei and E. Wang, *Chem. Soc. Rev.*, 2013, **42**, 6060-6093.

61.   L. F. Serafim, L. Wang, P. Rathee, J. Yang, H. S. Frenk Knaul and R. Prabhakar, *Curr. Opin. Green Sustain. Chem.*, 2021, **32**, 100529.

62.   M. J. Katz, R. C. Klet, S.-Y. Moon, J. E. Mondloch, J. T. Hupp and O. K. Farha, *ACS Catal.*, 2015, **5**, 4637-4642.

63.   J. Chin, *Acc. Chem. Res.*, 1991, **24**, 145-152.

64.   R. Breslow and S. D. Dong, *Chem. Rev.*, 1998, **98**, 1997-2012.

65.   J. Suh, *Acc. Chem. Res.*, 2003, **36**, 562-570.

66.   J. S. Johnson and D. A. Evans, *Acc. Chem. Res.*, 2000, **33**, 325-335.

67.   A. Pfaltz, *Acc. Chem. Res.*, 1993, **26**, 339-345.

68.   R. Beynon and J. S. Bond, *Proteolytic Enzymes*, Oxford University Press, New York, 2nd edn., 2001.

69.   J. K. Lassila, J. G. Zalatan and D. Herschlag, *Annu. Rev. Biochem.*, 2011, **80**, 669-702.

70.   J. Weston, *Chem. Rev.*, 2005, **105**, 2151-2174.

71.   T. Y. Lee and J. Suh, *Chem. Soc. Rev.*, 2009, **38**, 1949-1957.

72.   E. Meggers, *Chem. Comm.*, 2009, 1001-1010.

73.   L. J. Daumann, J. A. Larrabee, D. Ollis, G. Schenk and L. R. Gahan, *J. Inorg. Biochem.*, 2014, **131**, 1-7.

74.   E. Ghanem, Y. Li, C. Xu and F. M. Raushel, *Biochemistry*, 2007, **46**, 9032-9040.

75.   G. Schenk, I. Mateen, T.-K. Ng, M. M. Pedroso, N. Mitić, M. Jafelicci, R. F. C. Marques, L. R. Gahan and D. L. Ollis, *Coord. Chem. Rev.*, 2016, **317**, 122-131.

76.   A. M. Bezborodov and N. A. Zagustina, *Appl. Biochem. Microbiol.*, 2016, **52**, 237-249.

77.   Q. X. A. Sang, *Cell Res.*, 1998, **8**, 171-177.

78.   S. C. L. Kamerlin, P. K. Sharma, R. B. Prasad and A. Warshel, *Q Rev Biophys*, 2013, **46**, 1-132.

79.   K. Saha, U. M. R, J. Sikder, S. Chakraborty, S. S. da Silva and J. C. dos Santos, *Renew. Sust. Energ. Rev.*, 2017, **74**, 873-890.

80.   Y. Yu, X. Lou and H. Wu, *Energy & Fuels*, 2008, **22**, 46-60.

81.   S. Ügdüler, K. M. Van Geem, R. Denolf, M. Roosen, N. Mys, K. Ragaert and S. De Meester, *Green Chem.*, 2020, **22**, 5376-5394.

82.   J. Masbou, G. Drouin, S. Payraudeau and G. Imfeld, *Chemosphere*, 2018, **213**, 368-376.

83.   H. Lv, Y. V. Geletii, C. Zhao, J. W. Vickers, G. Zhu, Z. Luo, J. Song, T. Lian, D. G. Musaev and C. L. Hill, *Chem. Soc. Rev.*, 2012, **41**, 7572-7589.

84.   A. B. Bachman, D. Keramisanou, W. Xu, K. Beebe, M. A. Moses, M. V. Vasantha Kumar, G. Gray, R. E. Noor, A. van der Vaart, L. Neckers and I. Gelis, *Nat. Commun.*, 2018, **9**, 265.

85.   A. Radzicka and R. Wolfenden, *J. Am. Chem. Soc.*, 1996, **118**, 6105-6109.

86.   R. Wolfenden, *Annu. Rev. Biochem.*, 2011, **80**, 645-667.

87.   M. Paetzel, A. Karla, N. C. J. Strynadka and R. E. Dalbey, *Chem. Rev.*, 2002, **102**, 4549-4580.

88.   J. C. Powers, J. L. Asgian, Ö. D. Ekici and K. E. James, *Chem. Rev.*, 2002, **102**, 4639-4750.

89.   Y. Shen, Joachimiak, A., Rosner, M. R., and Tang, W-J., *Nature*, 2006, **443**, 870-874.

90.   N. Sträter and W. N. Lipscomb, *Biochemistry*, 1995, **34**, 9200-9210.

91.   W. N. Lipscomb and N. Sträter, *Chem. Rev.*, 1996, **96**, 2375-2434.

92.   T. Devamani, A. M. Rauwerdink, M. Lunzer, B. J. Jones, J. L. Mooney, M. A. O. Tan, Z.-J. Zhang, J.-H. Xu, A. M. Dean and R. J. Kazlauskas, *J. Am. Chem. Soc.*, 2016, **138**, 1046-1056.

93.   T. J. Paul, A. Barman, M. Ozbil, R. P. Bora, T. Zhang, G. Sharma, Z. Hoffmann and R. Prabhakar, *Phys. Chem. Chem. Phys.*, 2016, **18**, 24790-24801.

94.   B. Turk, *Nat. Rev. Drug Discov.*, 2006, **5**, 785-799.

95.   L. Tong, *Chem. Rev.*, 2002, **102**, 4609-4626.

96.   P. Fitzgerald and J. Springer, *Annual Review of Biophysics and Biophysical Chemistry*, 1991, **20**, 299-320.

97.   H. Daver, B. Das, E. Nordlander and F. Himo, *Inorg. Chem.*, 2016, **55**, 1872-1882.

98.   C. I. Maxwell, N. J. Mosey and R. Stan Brown, *J. Am. Chem. Soc.*, 2013, **135**, 17209-17222.

99.   D. L. Collins-Wildman, M. Kim, K. P. Sullivan, A. M. Plonka, A. I. Frenkel, D. G. Musaev and C. L. Hill, *ACS Catal.*, 2018, **8**, 7068-7076.

100.   M. M. Aboelnga and S. D. Wetmore, *J. Am. Chem. Soc.*, 2019, **141**, 8646-8656.

101.   X. López, J. J. Carbó, C. Bo and J. M. Poblet, *Chem. Soc. Rev.*, 2012, **41**, 7537-7571.

102.   A. B. Becker, and Roth, R. A., *Proc. Natl. Acad. Sci.*, 1992, **89**, 3835-3839.

103.   R. K. Perlman, and Rosner, M. R., *J. Biol. Chem.*, 1994, **269**, 33140–33145.

104.   D. R. Holland, Hausrath, A. C., Juers, D., and Matthews, B. W., *Protein Sci.*, 1995, **4**, 1955-1965.

105.   F. A. Quiocho, C. H. McMurray and W. N. Lipscomb, *Proc. Natl. Acad. Sci. U.S.A.* , 1972, **69**, 2850-2854.

106.   B. W. Matthews, Schoenbo.Bp, Dupourqu.D, Jansoniu.Jn and P. M. Colman, *Nat. New Biol.*, 1972, **238**, 37-&.

107.   W. Q. Qiu and M. F. Folstein, *Neurobiol. Aging*, 2006, **27**, 190-198.

108.   G. Taubes, *Science*, 2003, **301**, 40–41.

109.   E. Malito, R. E. Hulse and W. J. Tang, *Cellular and molecular life sciences : CMLS*, 2008, **65**, 2574-2585.

110.   H. Im, Manolopoulou, M., Malito, E., Shen, Y., Zhao, J., Neant-Fery, M., Sun, C-Y, Meredith, S. C., Sisodia, S. S., Leissering, M. A., and Tang, W-J., *J. Biol. Chem.*, 2007, **282**, 25453-25463.

111.   N. Iwata, S. Tsubuki, Y. Takaki, K. Shirotani, B. Lu, N. P. Gerard, C. Gerard, E. Hama, H.-J. Lee and T. C. Saido, *Science*, 2001, **292**, 1550-1552.

112.   J. A. Carson and A. J. Turner, *J. Neurochem.*, 2002, **81**, 1-8.

113.   A. J. Turner, C. D. Brown, J. A. Carson and K. Barnes, *Cellular Peptidases in Immune Functions and Diseases 2*, 2002, 229-240.

114.   I. Bertini, Calderone, V., Fragai, M., Luchinat, C., Maletta, M., and Yeo, K. J., *Angew. Chem. Int. Ed.*, 2006, **45**, 7952-7955.

115.   M. F. Browner, Smith, W. W., and Castelhano, A. L., *Biochemistry*, 1995, **34**, 6602-6610.

116.   A. Heinz, M. C. Jung, L. Duca, W. Sippl, S. Taddese, C. Ihling, A. Rusciani, G. Jahreis, A. S. Weiss and R. H. Neubert, *FEBS J.*, 2010, **277**, 1939-1956.

117.   H.-J. Ra, S. Harju-Baker, F. Zhang, R. J. Linhardt, C. L. Wilson and W. C. Parks, *J. Biol. Chem.*, 2009, **284**, 27924-27932.

118.   D. N. Silverman and S. Lindskog, *Acc. Chem. Res.*, 1988, **21**, 30-36.

119.   V. M. Krishnamurthy, G. K. Kaufman, A. R. Urbach, I. Gitlin, K. L. Gudiksen, D. B. Weibel and G. M. Whitesides, *Chem. Rev.*, 2008, **108**, 946-1051.

120.   M. Tauro, J. McGuire and C. C. Lynch, *Cancer Metastasis Rev.*, 2014, **33**, 1043-1057.

121.   D. A. Siwik, P. J. Pagano and W. S. Colucci, *Am. J. Physiol. Cell Physiol.*, 2001, **280**, C53-C60.

122.   A. Taylor, *FASEB J.*, 1993, **7**, 290-298.

123.   H. I. Park and L. J. Ming, *Angew. Chem. Int. Ed.*, 1999, **38**, 2914-2916.

124.   A. Ercan, H. I. Park and L. J. Ming, *Biochemistry*, 2006, **45**, 13779-13793.

125.   H. Vahrenkamp, *Dalton Trans.*, 2007, DOI: 10.1039/B712138E, 4751-4759.

126.   A. D. Becke, *J. Chem. Phys.*, 1993, **98**, 5648-5652.

127.   C. Lee, W. Yang and R. G. Parr, *Phys. Rev. B*, 1988, **37**, 785-789.

128. C. Adamo and V. Barone, *J. Chem. Phys.*, 1998, **108**, 664-675.

129. Y. Zhao and D. G. Truhlar, *Theor. Chem. Acc.*, 2008, **120**, 215-241.

130. A. Glades and B. L. Vallee, *Metal Ions in Biological Systems*, Dekker, New York, 1983.

131. V. Pelmenschikov, M. R. Blomberg and P. E. Siegbahn, *J. Biol. Inorg. Chem.*, 2002, **7**, 284-298.

132. N. M. Hooper, *FEBS Lett.*, 1994, **354**, 1-6.

133. H. Neurath, *Science*, 1984, **224**, 350-357.

134. L. E. Sanman and M. Bogyo, *Annu. Rev. Biochem.*, 2014, **83**, 249-273.

135. R. P. Bora, M. Ozbil and R. Prabhakar, *J. Biol. Inorg. Chem.*, 2010, **15**, 485-495.

136. K. Morihara, and Hiroshige, T., *Eur. J. Biochem.*, 1970, **15**, 374-380.

137. Q. Hu, V. M. Jayasinghe-Arachchige and R. Prabhakar, *J. Chem. Inf. Model.*, 2021, **61**, 764-776.

138. M. F. Browner, W. W. Smith and A. L. Castelhano, *Biochemistry*, 1995, **34**, 6602-6610.

139. R. P. Bora, A. Barman, X. Zhu, M. Ozbil and R. Prabhakar, *J. Phys. Chem. B*, 2010, **114**, 10860–10875.

140. X. Zhu, A. Barman, M. Ozbil, T. Zhang, S. Li and R. Prabhakar, *J. Biol. Inorg. Chem.*, 2012, **17**, 209-222.

141. S.-L. Chen, T. Marino, W.-H. Fang, N. Russo and F. Himo, *J. Phys. Chem. B*, 2008, **112**, 2494-2500.

142. M. Leopoldini, N. Russo and M. Toscano, *J. Am. Chem. Soc.*, 2007, **129**, 7776-7784.

143. M. E. Alberto, M. Leopoldini and N. Russo, *Inorg. Chem.*, 2011, **50**, 3394-3403.

144. M. P. Allen, A. H. Yamada and F. H. Carpenter, *Biochemistry*, 1983, **22**, 3778-3783.

145.   L. F. Serafim, V. M. Jayasinghe-Arachchige, L. Wang and R. Prabhakar, *J. Chem. Inf. Model.*, 2022, **62**, 2466-2480.

146.   Y. F. Hershcovitz, R. Gilboa, V. Reiland, G. Shoham and Y. Shoham, *FEBS J.*, 2007, **274**, 3864-3876.

147.   Y. Fundoiano-Hershcovitz, L. Rabinovitch, Y. Langut, V. Reiland, G. Shoham and Y. Shoham, *FEBS Lett.*, 2004, **571**, 192-196.

148.   C. C. Huang, C. V. Smith, M. S. Glickman, W. R. Jacobs and J. C. Sacchettini, *J. Biol. Chem.*, 2002, **277**, 11559-11569.

149.   F. Courtois and O. Ploux, *Biochemistry*, 2005, **44**, 13583-13590.

150.   N. Sträter, L. Sun, E. R. Kantrowitz and W. N. Lipscomb, *Proc. Natl. Acad. Sci. U.S.A.*, 1999, **96**, 11151-11155.

151.   N. M. Milović and N. M. Kostić, *J. Am. Chem. Soc.*, 2003, **125**, 781-788.

152.   R. Bakhtiar, J. J. Thomas and G. Siuzdak, *Acc. Chem. Res.*, 2000, **33**, 179-187.

153.   M. Fountoulakis and H.-W. Lahm, *J. Chromatogr. A*, 1998, **826**, 109-134.

154.   N. E. Wezynfeld, T. Frączyk and W. Bal, *Coord. Chem. Rev.*, 2016, **327-328**, 166-187.

155.   Q. Li, L. Yi, P. Marek and B. L. Iverson, *FEBS Lett.*, 2013, **587**, 1155-1163.

156.   N. M. Milovic, and Kostić, N. M., *J. Am. Chem. Soc.*, 2002, **125**, 781-788.

157.   A. Kumar, Zhu, X., Walsh, K., and Prabhakar, R., *Inorg. Chem.*, 2010, **49**, 38-46.

158.   T. C. Bruice, Tsubouchi, A., Dempcy, R. O., and Olson, L. P., *J. Am. Chem. Soc.*, 1996, **118**, 9867-9875.

159.   E. Hegg, L.; Burstyn, J., N., *Coord. Chem. Rev.*, 1998, **173**, 133-165.

160.   C. Liu, Wang, M., Zhang, T., and Sun, H., *Coord. Chem. Rev.*, 2004, **248**, 147-168.

161.   N. M. Milović, J. D. Badjić and N. M. Kostić, *J. Am. Chem. Soc.*, 2004, **126**, 696-697.

162.   R. Breslow and L. E. Overman, *J. Am. Chem. Soc.*, 1970, **92**, 1075-1077.

163.   T. Zhang, X. Zhu and R. Prabhakar, *J. Phys. Chem. B*, 2014, **118**, 4106-4114.

164.   H. Kim, B. Jang, Y. Cheon, M. Suh and J. Suh, *J. Biol. Inorg. Chem.*, 2009, **14**, 151-157.

165.   J. Suh, S. H. Yoo, M. G. Kim, K. Jeong, J. Y. Ahn, M.-s. Kim, P. S. Chae, T. Y. Lee, J. Lee, J. Lee, Y. A. Jang and E. H. Ko, *Angew. Chem. Int. Ed. Engl.*, 2007, **46**, 7064-7067.

166.   W. Chei, H. Ju and J. Suh, *J. Biol. Inorg. Chem.*, 2011, **16**, 511-519.

167.   S. W. Jang and J. Suh, *Org. Lett.*, 2008, **10**, 481-484.

168.   J. W. Jeon, S. J. Son, C. E. Yoo, I. S. Hong and J. Suh, *Bioorg. Med. Chem.*, 2003, **11**, 2901-2910.

169.   T. Zhang, X. Zhu and R. Prabhakar, *Organometallics*, 2014, **33**, 1925-1935.

170.   B. Jang and J. Suh, *Bull. Korean Chem. Soc.*, 2008, **29**, 202-204.

171.   T. Zhang, G. Sharma, T. J. Paul, Z. Hoffmann and R. Prabhakar, *J. Chem. Inf. Model.*, 2017, **57**, 1079-1088.

172.   J. C. M. Rivas, E. Salvagni, R. Prabaharan, R. T. M. Rosales and S. Parsons, *Dalton Trans.*, 2004, 172-177.

173.   M. Kassai, R. G. Ravi, S. J. Shealy and K. B. Grant, *Inorg. Chem.*, 2004, **43**, 6130-6132.

174.   K. Stroobants, E. Moelants, H. G. T. Ly, P. Proost, K. Bartik and T. N. Parac-Vogt, *Chem. Eur. J.*, 2013, **19**, 2848-2858.

175.   A. Sap, L. Van Tichelen, A. Mortier, P. Proost and T. N. Parac-Vogt, *Eur. J. Inorg. Chem.*, 2016, **2016**, 5098-5105.

176.   H. G. T. Ly and T. N. Parac-Vogt, *Chemphyschem*, 2017, **18**, 2451-2458.

177.   K. Stroobants, V. Goovaerts, G. Absillis, G. Bruylants, E. Moelants, P. Proost and T. N. Parac-Vogt, *Chem. Eur. J.*, 2014, **20**, 9567-9577.

178. K. Stroobants, G. Absillis, E. Moelants, P. Proost and T. N. Parac-Vogt, *Chem. Eur. J.*, 2014, **20**, 3894-3897.

179. G. Sudlow, D. J. Birkett and D. N. Wade, *Mol. Pharmacol.*, 1975, **11**, 824-832.

180. G. Sudlow, D. J. Birkett and D. N. Wade, *Mol. Pharmacol.*, 1976, **12**, 1052-1061.

181. S. Baroni, M. Mattu, A. Vannini, R. Cipollone, S. Aime, P. Ascenzi and M. Fasano, *Eur. J. Biochem.*, 2001, **268**, 6214-6220.

182. A. di Masi, F. Gullotta, A. Bolli, G. Fanali, M. Fasano and P. Ascenzi, *FEBS J.*, 2011, **278**, 654-662.

183. T. J. Paul, T. N. Parac-Vogt, D. Quiñonero and R. Prabhakar, *J. Phys. Chem. B*, 2018, **122**, 7219-7232.

184. J. L. Knight and C. L. Brooks, 3rd, *J. Comput. Chem.*, 2009, **30**, 1692-1700.

185. X. Kong and C. L. B. III, *J. Chem. Phys.*, 1996, **105**, 2414-2423.

186. Z. Guo, C. L. Brooks and X. Kong, *J. Phys. Chem. B*, 1998, **102**, 2032-2036.

187. V. M. Jayasinghe-Arachchige, Q. Hu, G. Sharma, T. J. Paul, M. Lundberg, D. Quinonero, T. N. Parac-Vogt and R. Prabhakar, *J. Comput. Chem.*, 2019, **40**, 51-61.

188. H. G. T. Ly, G. Absillis and T. N. Parac-Vogt, *New J. Chem.*, 2016, **40**, 976-984.

189. J. A. Gerlt and F. H. Westheimer, *J. Am. Chem. Soc.*, 1973, **95**, 8166-8168.

190. J. A. Gerlt and G. J. Whitman, *J. Biol. Chem.*, 1975, **250**, 5053-5058.

191. L. J. Daumann, B. Y. McCarthy, K. S. Hadler, T. P. Murray, L. R. Gahan, J. A. Larrabee, D. L. Ollis and G. Schenk, *Biochim. Biophys. Acta. Proteins Proteom BBA-PROTEINS PROTEOM*, 2013, **1834**, 425-432.

192. K. S. Hadler, N. Mitić, F. Ely, G. R. Hanson, L. R. Gahan, J. A. Larrabee, D. L. Ollis and G. Schenk, *J. Am. Chem. Soc.*, 2009, **131**, 11900-11908.

193.	E. Ghanem and F. M. Raushel, *Toxicol. Appl. Pharmacol.*, 2005, **207**, 459-470.

194.	C. J. Jackson, K. S. Hadler, P. D. Carr, A. J. Oakley, S. Yip, G. Schenk and D. L. Ollis, *Acta Crystallogr. F*, 2008, **64**, 681-685.

195.	T. J. Paul, G. Schenk and R. Prabhakar, *J. Phys. Chem. B*, 2018, **122**, 5797-5808.

196.	M. M. Pedroso, F. Ely, M. C. Carpenter, N. a. Mitić, L. R. Gahan, D. L. Ollis, D. E. Wilcox and G. Schenk, *Biochemistry*, 2017, **56**, 3328-3336.

197.	K. S. Hadler, N. Mitic, S. H.-C. Yip, L. R. Gahan, D. L. Ollis, G. Schenk and J. A. Larrabee, *Inorg. Chem.*, 2010, **49**, 2727-2734.

198.	A. Ercan, W. M. Tay, S. H. Grossman and L.-J. Ming, *J. Inorg. Biochem.*, 2010, **104**, 19-29.

199.	R. M. O'Ferrall, *J. Chem. Soc. B*, 1970, 274-277.

200.	A. J. Kirby and F. Nome, *Acc. Chem. Res.*, 2015, **48**, 1806-1814.

201.	F. Duarte, J. Åqvist, N. H. Williams and S. C. Kamerlin, *J. Am. Chem. Soc.*, 2014, **137**, 1081-1093.

202.	M. E. Alberto, G. Pinto, N. Russo and M. Toscano, *Chem. Eur. J.*, 2015, **21**, 3736-3745.

203.	V. López-Canut, M. Roca, J. Bertrán, V. Moliner and I. a. Tuñón, *J. Am. Chem. Soc.*, 2010, **132**, 6955-6963.

204.	M. Klähn, E. Rosta and A. Warshel, *J. Am. Chem. Soc.*, 2006, **128**, 15310-15323.

205.	A. N. Bigley and F. M. Raushel, *Biochim. Biophys. Acta. Proteins Proteom BBA-PROTEINS PROTEOM*, 2013, **1834**, 443-453.

206.	T. Klabunde, N. Sträter, R. Fröhlich, H. Witzel and B. Krebs, *J. Mol. Biol.*, 1996, **259**, 737-748.

207.	S. D. Aubert, Y. Li and F. M. Raushel, *Biochemistry*, 2004, **43**, 5707-5715.

208.   H. Zhang, L. Yang, W. Ding and Y. Ma, *J. Biol. Inorg. Chem.*, 2018, **23**, 277-284.

209.   D. Roston and Q. Cui, *J. Am. Chem. Soc.*, 2016, **138**, 11946-11957.

210.   G. Sharma, V. M. Jayasinghe-Arachchige, Q. Hu, G. Schenk and R. Prabhakar, *ACS Catal.*, 2020, **10**, 3684-3696.

211.   G. Sharma, Q. Hu, V. Jayasinghe-Arachchige, T. Paul, G. Schenk and R. Prabhakar, *Phys. Chem. Chem. Phys.*, 2019, 5499-5509.

212.   M. E. Alberto, T. Marino, M. J. Ramos and N. Russo, *J. Chem. Theory Comput.*, 2010, **6**, 2424-2433.

213.   R. Z. Liao, F. Himo, J. G. Yu and R. Z. Liu, *Eur. J. Inorg. Chem.*, 2009, **2009**, 2967-2972.

214.   H. Zhang, Y. Ma and J.-G. Yu, *J. Biol. Inorg. Chem.*, 2013, **18**, 1019-1026.

215.   H. M. Greenblatt, O. Almog, B. Maras, A. Spungin-Bialik, D. Barra, S. Blumberg and G. Shoham, *J. Mol. Biol.*, 1997, **265**, 620-636.

216.   T. Koike and E. Kimura, *J. Am. Chem. Soc.*, 1991, **113**, 8935-8941.

217.   Y. Li, X.-M. Lu, X. Sheng, G.-Y. Lu, Y. Shao and Q. Xu, *J. Incl. Phenom. Macrocycl. Chem.*, 2007, **59**, 91-98.

218.   U. Baykal, M. S. Akkaya and E. U. Akkaya, *J. Incl. Phenom. Macrocycl. Chem.*, 1999, **35**, 311-315.

219.   P. Gómez-Tagle and A. K. Yatsimirsky, *Inorg. Chem.*, 2001, **40**, 3786-3796.

220.   N. W. Luedtke and A. Schepartz, *Chem. Comm.*, 2005, 5426-5428.

221.   J. Rammo, R. Hettich, A. Roigk and H.-J. Schneider, *Chem. Comm.*, 1996, 105-107.

222.   S. J. Franklin, *Curr. Opin. Chem. Biol.*, 2001, **5**, 201-208.

223.   Q. Hu, V. M. Jayasinghe-Arachchige, J. Zuchniarz and R. Prabhakar, *Front. Chem.*, 2019, **7**.

224.   A. Neves, M. Lanznaster, A. J. Bortoluzzi, R. A. Peralta, A. Casellato, E. E. Castellano, P. Herrald, M. J. Riley and G. Schenk, *J. Am. Chem. Soc.*, 2007, **129**, 7486-7487.

225.   D. Montagner, V. Gandin, C. Marzano and A. Erxleben, *J. Inorg. Biochem.*, 2015, **145**, 101-107.

226.   D. Montagner, V. Gandin, C. Marzano and A. Erxleben, *Eur. J. Inorg. Chem.*, 2014, **2014**, 4084-4092.

227.   V. M. Jayasinghe-Arachchige, L. F. Serafim, Q. Hu, C. Ozen, S. N. Moorkkannur, G. Schenk and R. Prabhakar, *ACS Catal.*, 2023, **13**, 3131-3147.

228.   J. N. Harvey, F. Himo, F. Maseras and L. Perrin, *ACS Catal.*, 2019, **9**, 6803-6813.

229.   O. A. von Lilienfeld, K.-R. Müller and A. Tkatchenko, *Nat. Rev. Chem.*, 2020, **4**, 347-358.

230.   P. C. St. John, Y. Guan, Y. Kim, S. Kim and R. S. Paton, *Nat. Commun.*, 2020, **11**, 2328.
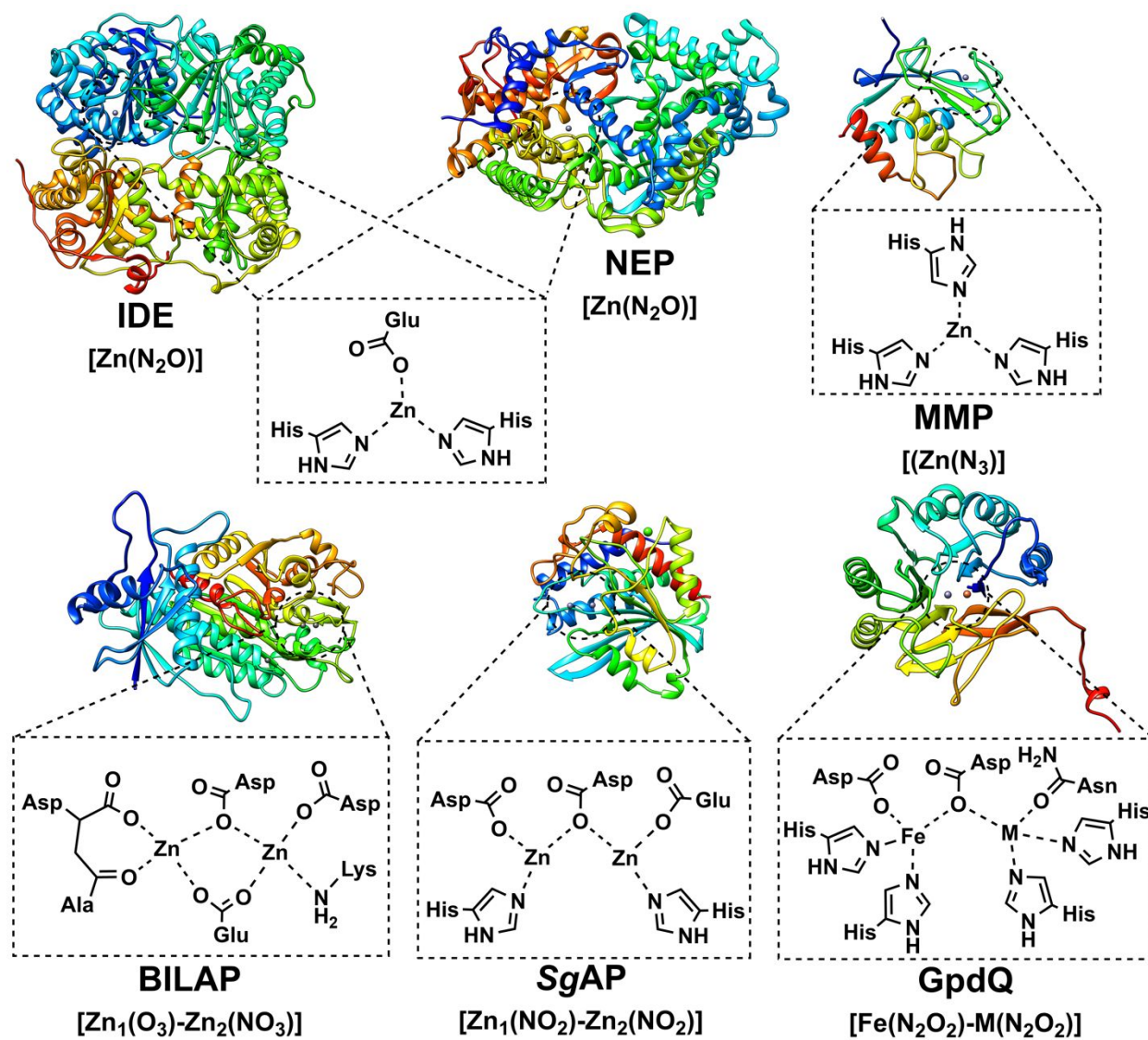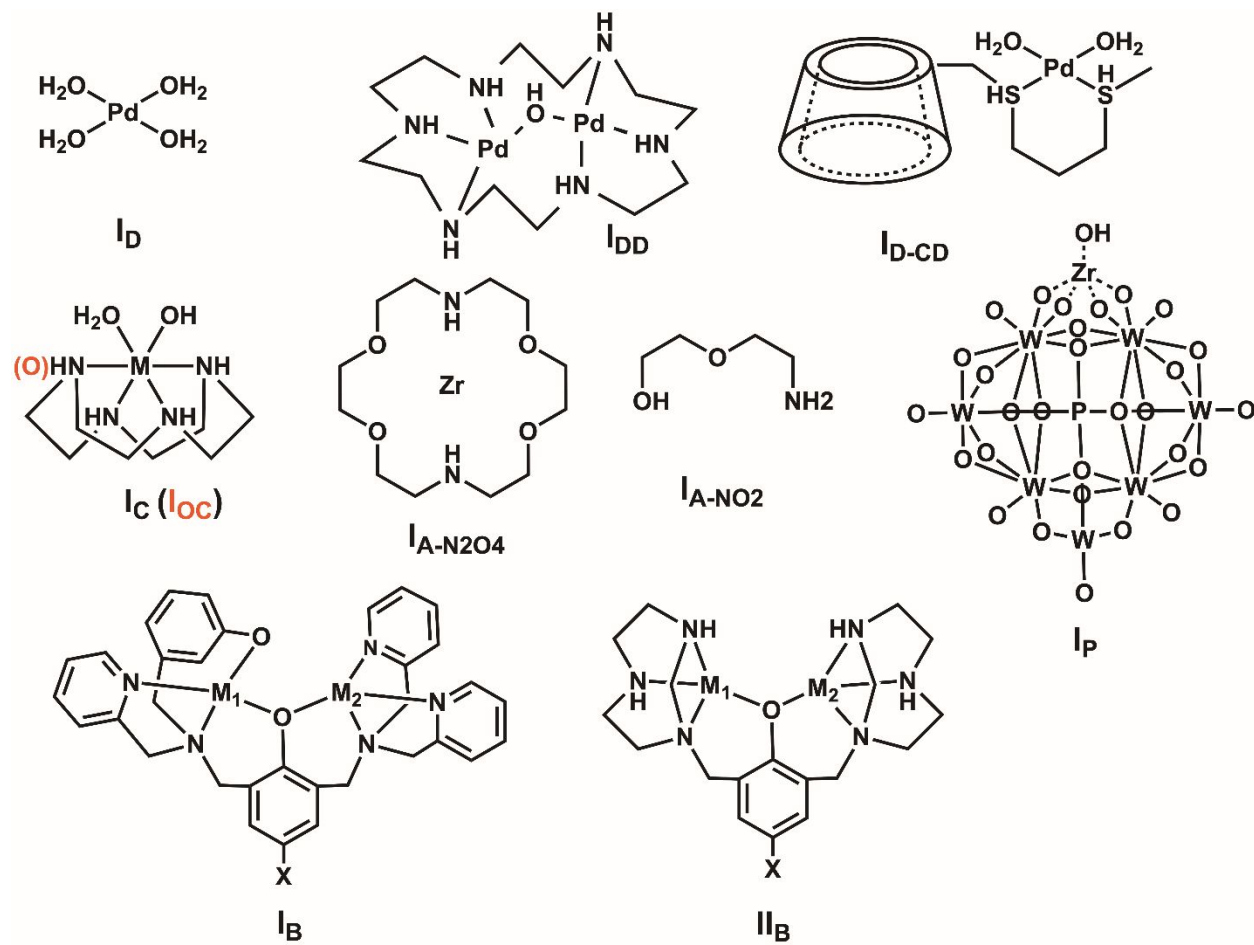
Figure 1: Metal center(s) of mono- and binuclear metallohydrolases.
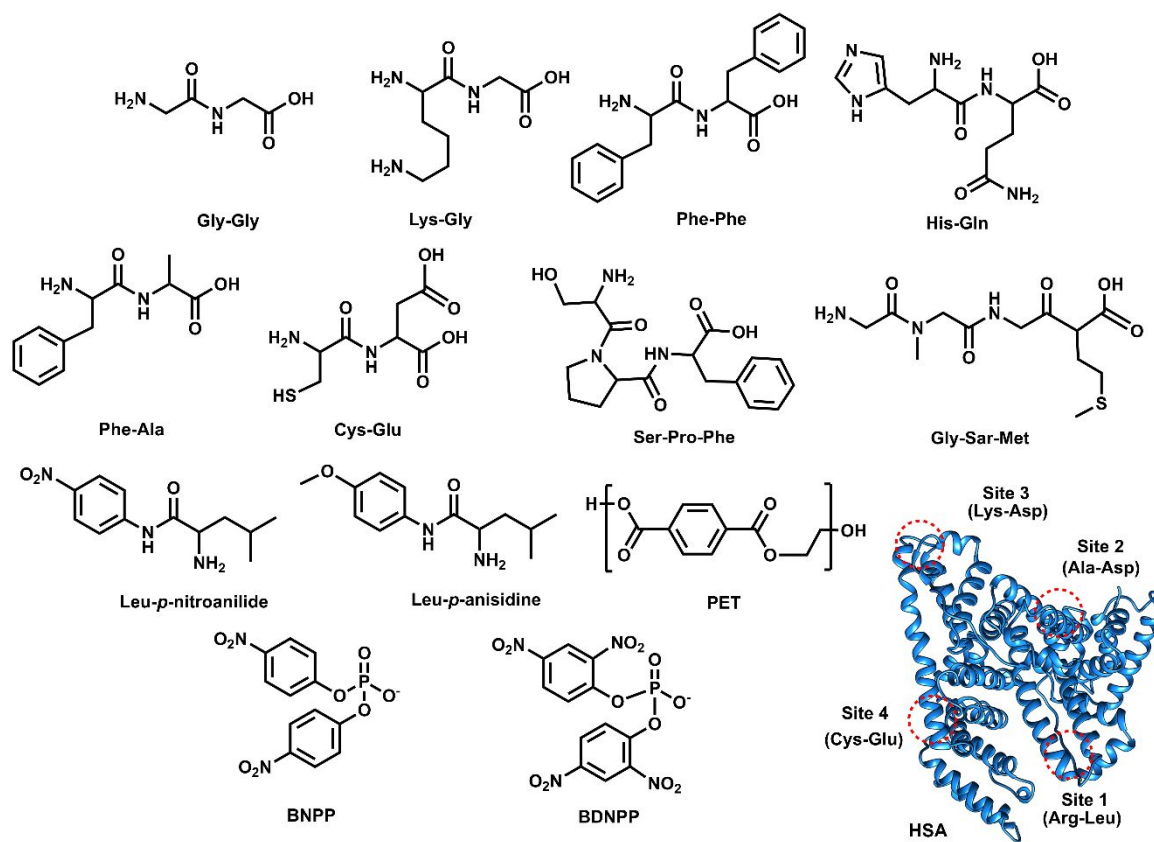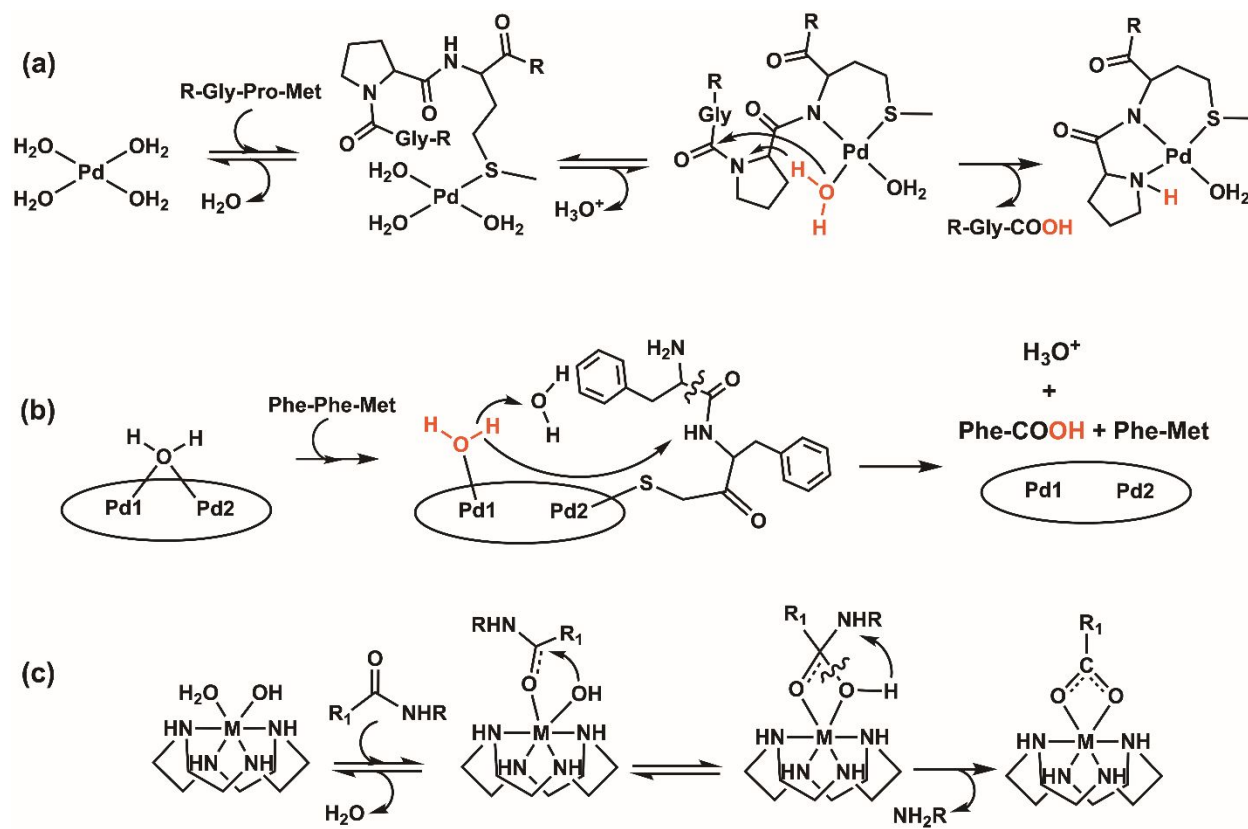
Figure 2: Structures of the substrates used for peptide, ester and phosphoester hydrolysis.
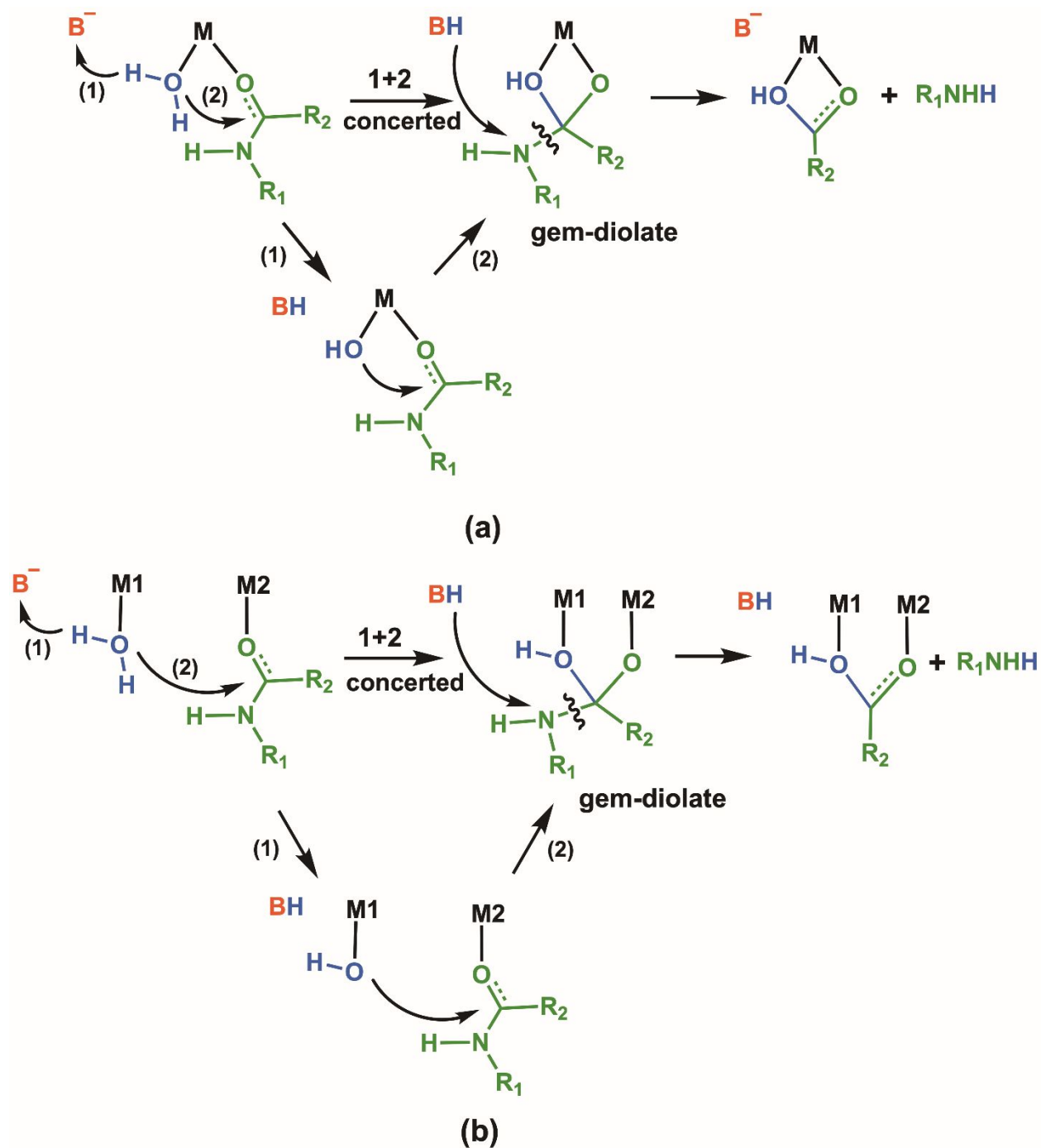
Figure 3: General mechanisms of peptide hydrolysis for mononuclear (a) and binuclear (b) systems.
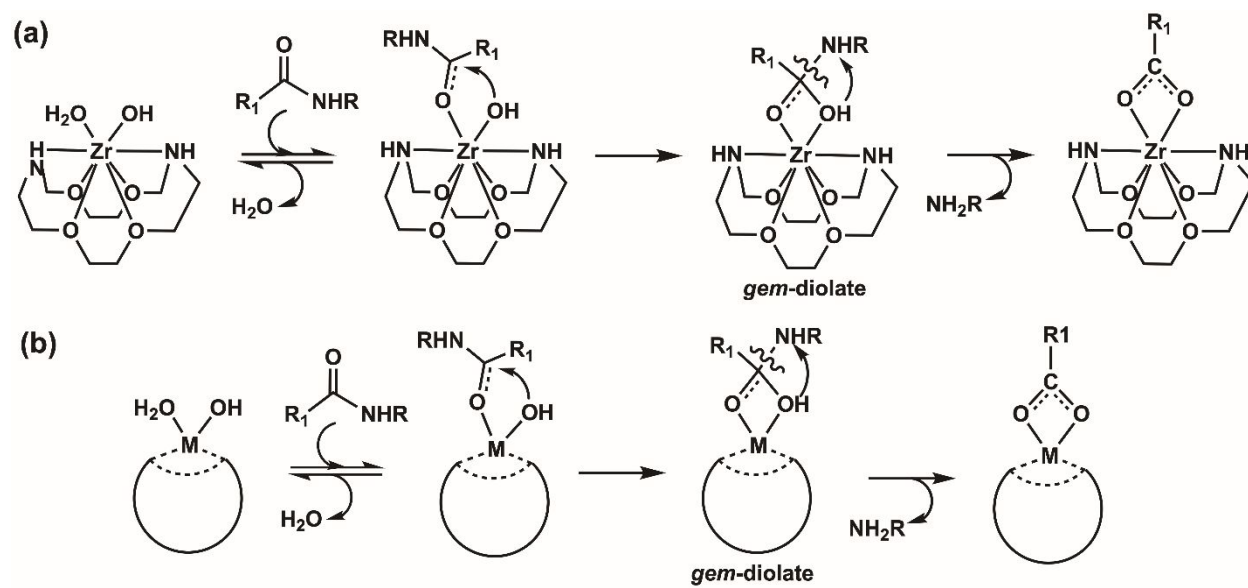
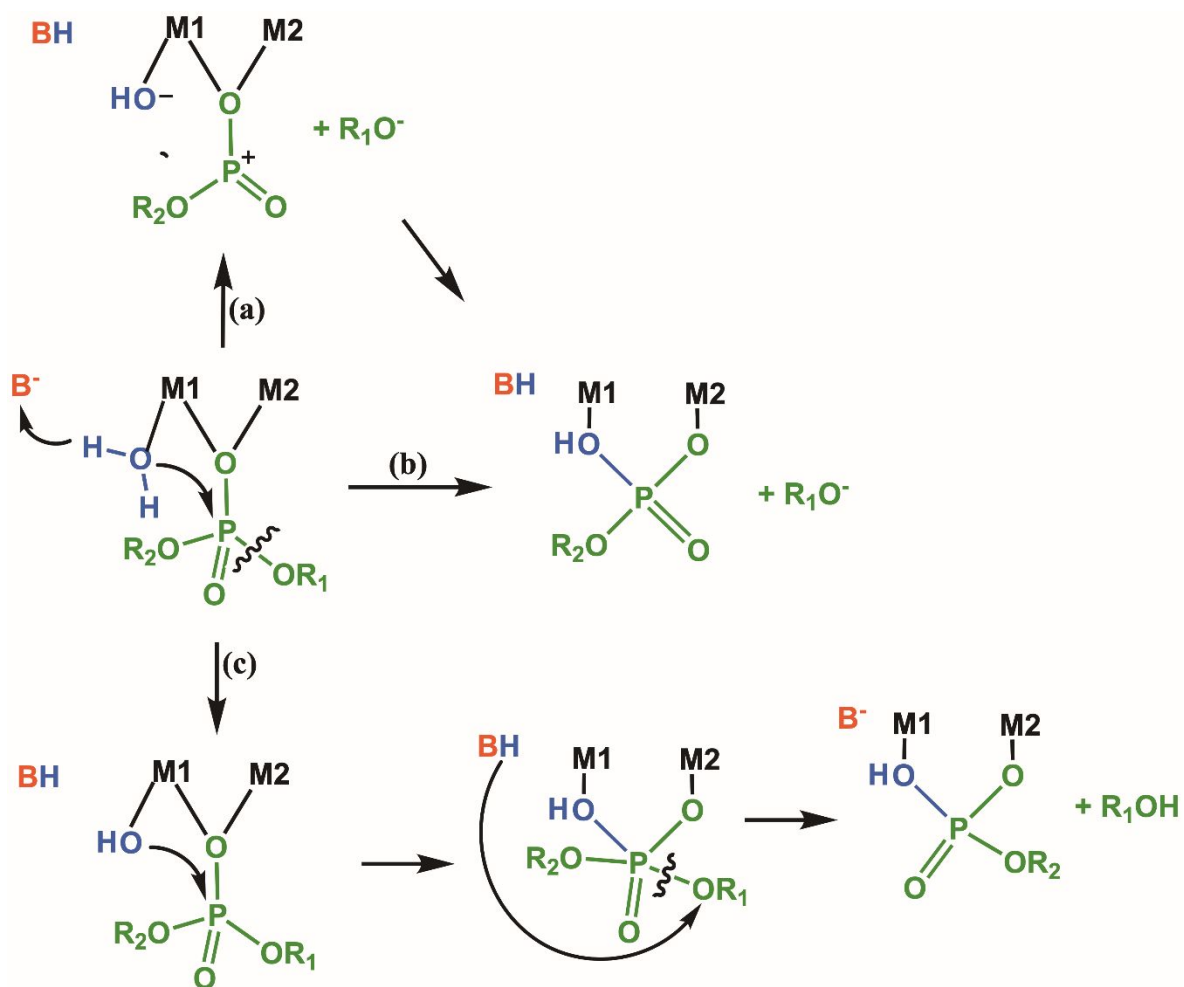**Figure 4:** Structures of the metal complexes used for peptide, ester and phosphoester hydrolysis

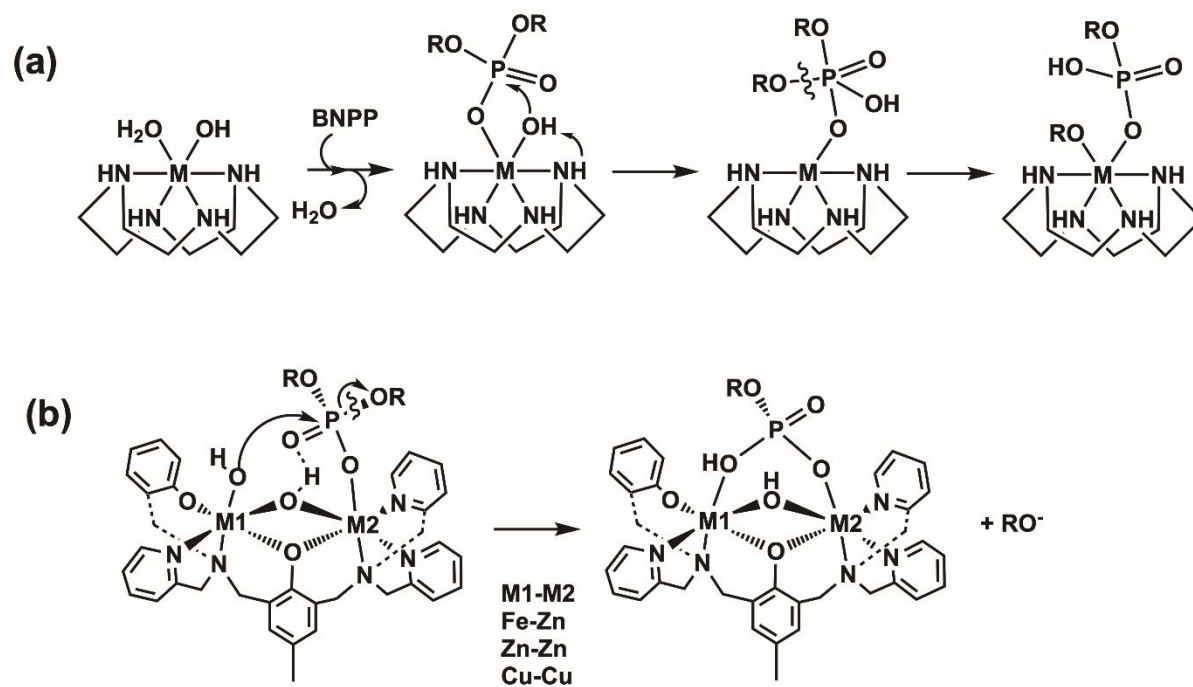**Figure 5:** Mechanisms of peptide hydrolysis employed by metal complexes (a) $\mathbf{I_D}$, (b) $\mathbf{I_{DD}}$ and (c) $\mathbf{I_C}$.

Figure 6: Mechanisms of peptide hydrolysis employed by metal complexes (a) $\mathbf{I_A}$ and (b) $\mathbf{I_P}$.

Figure 7: General mechanisms of phosphoester hydrolysis employed by binuclear systems.

Figure 8: Mechanisms of phosphoester hydrolysis employed by metal complexes (a) I_C and (b)

I_B.